Article

Noncovalent Interactions under Extreme Conditions: High-Pressure and Low-Temperature Diffraction Studies of the Isostructural Metal#Organic Networks (4-Chloropyridinium) [CoX] (X = Cl, Br)

Guillermo Mínguez Espallargas, Lee Brammer, David R.
Allan, Colin R. Pulham, Neil Robertson, and John E. Warren

More About This Article

Additional resources and features associated with this article are available within the HTML version:

- Supporting Information
- Links to the 2 articles that cite this article, as of the time of this article download
- Access to high resolution figures
- Links to articles and content related to this article
- Copyright permission to reproduce figures and/or text from this article

View the Full Text HTML

Noncovalent Interactions under Extreme Conditions: High-Pressure and Low-Temperature Diffraction Studies of the Isostructural Metal−Organic Networks (4-Chloropyridinium)₂[CoX₄] (X = Cl, Br)

Guillermo Mínguez Espallargas,[†] Lee Brammer,*,[†] David R. Allan,[‡,§]
Colin R. Pulham,[‡] Neil Robertson,[‡] and John E. Warren[∥]

Department of Chemistry, University of Sheffield, Sheffield S3 7HF, U.K., School of Chemistry, University of Edinburgh, King's Buildings, Edinburgh EH9 3JJ, U.K., Diamond Light Source, STFC Rutherford Appleton Laboratory, Chilton, Didcot, Oxon OX11 0QX, U.K., and Synchrotron Radiation Source, STFC Daresbury Laboratory, Daresbury, Warrington WA4 4AD, U.K.

Received February 15, 2008; E-mail: lee.brammer@sheffield.ac.uk

Abstract: The crystal structures of the two isostructural metal−organic salts, (4-chloropyridinium)₂[CoX₄], X = Cl (**1**), Br (**2**), have each been determined at nine temperatures from 30 to 300 K and at nine pressures from atmospheric pressure to 4.2 GPa. A 5% reduction in unit cell volume is observed upon temperature reduction, whereas an 18−19% reduction is observed upon increasing the pressure over the ranges studied. The structures adopt a tape arrangement propagated by bifurcated N−H···X₂Co hydrogen bonds and by Co−X···Cl−C halogen bonds. Intertape interactions include type I Co−X···Cl−C and C−Cl···Cl−C halogen−halogen interactions as well as offset π-stacking between the aromatic rings of the cations. Although little anisotropy in compression is seen upon temperature reduction, marked anisotropy in compression is observed upon pressure increase. Compression between tapes far exceeds compression along the tape, consistent with the strong attractive nature of the intratape N−H···X₂Co and Co−X···Cl−C interactions and the weaker dispersion dominated Co−X···Cl−C and C−Cl···Cl−C halogen−halogen interactions and π-stacking interactions. Increased distortion of the [CoX₄]²⁻ anions from idealized tetrahedral geometry arises upon pressure increase, consistent with local changes in the electric field that result from compression of the pairs of π-stacked cations. The study of the isostructural pair of compounds permits a rare opportunity for quantitative evaluation of the "internal" or "chemical" pressure exerted by changing the [CoBr₄]²⁻ anion for the smaller [CoCl₄]²⁻ anion. Thus, crystal structures of **1** and **2** with equivalent unit cell volumes require an additional pressure of ca. 1 GPa exerted upon the structure containing the larger [CoBr₄]²⁻ anion (**2**). This internal pressure increases to ca. 1.9 GPa at the highest pressures used in this study. Most significant is that examination of the isovolumetric pairs of structures shows that the structures containing the [CoCl₄]²⁻ anion are contracted along the <10$\bar{1}$> vector, the direction of tape propagation, by ca. 1.2% and correspondingly expanded in other directions, relative to those containing the [CoBr₄]²⁻ anion. Since the effect of difference in anion size has been removed by application of pressure, this anisotropy in dimensions clearly indicates that the N−H···X₂Co hydrogen bonds and Co−X···Cl−C halogen bonds are more strongly attractive for X = Cl rather than X = Br. Use of internal pressure thereby provides unique insight into the relative strength of intermolecular interactions.

Introduction

Molecules in crystals are arranged to maximize the attractive interactions and minimize the repulsive ones. Thus, the distance between two atoms corresponds to the equilibrium between attractive and repulsive forces: electrostatic, charge transfer, polarization, dispersive, and exchange interactions.[1] The development of accurate atom−atom potentials that can explain interatomic interactions in molecular crystals is currently of

much interest,[2,3] largely driven by a desire to predict stability and physical properties of new crystal forms of pharmaceuticals.[4] However, such understanding has the potential to provide

---

† University of Sheffield.
‡ University of Edinburgh.
§ STFC Rutherford Appleton Laboratory.
∥ STFC Daresbury Laboratory.
(1) Dance, I. *New J. Chem.* **2003**, *27*, 22.

(2) (a) Karamertzanis, P. G.; Anandamanoharan, P. R.; Fernandes, P.; Cains, P. W.; Vickers, M.; Tocher, D. A.; Florence, A. J.; Price, S. L. *J. Phys. Chem. B* **2007**, *111*, 5326. (b) Karamertzanis, P. G.; Price, S. L. *J. Chem. Theory Comput.* **2006**, *2*, 1184. (c) Price, S. L. *CrystEngComm* **2004**, *6*, 344. (d) Day, G. M.; Price, S. L. *J. Am. Chem. Soc.* **2003**, *125*, 16434.

(3) (a) Gavezzotti, A. *CrystEngComm* **2003**, *5*, 429. (b) Gavezzotti, A. *CrystEngComm* **2003**, *5*, 439. (c) Gavezzotti, A. *J. Phys. Chem. B* **2003**, *107*, 2344. (d) Gavezzotti, A. *J. Phys. Chem. B* **2002**, *106*, 4145.

(4) (a) Vippagunta, S. R.; Brittain, H. G.; Grant, D. J. W. *Adv. Drug Delivery Rev.* **2001**, *48*, 3. (b) Price, S. L. *Adv. Drug Delivery Rev.* **2004**, *56*, 301.

important input into the more extensive field of molecular materials design by crystal engineering approaches.[5,6]

Data on the compressibility of noncovalent interactions with temperature enhance our understanding of these interactions and provide quantitative input to improve the parameters used to describe the intermolecular interaction potentials in molecular crystals, since the temperature dependence of the distance between a pair of nonbonded atoms is expected to be inversely related to the strength of the interaction.[7] For a strong interaction, a small variation in the distance produces a large increase in the energy since the potential well is relatively deep. On the other hand, in weak interactions, which have a shallow potential well, variation of the distance does not cost much in energy, permitting greater deformation with change in temperature.

Exploration of such changes using variable-temperature crystallographic experiments has been mostly performed for the study of hydrogen-bonded systems.[8] The variation of the hydrogen bond distance with temperature has been examined,[9] as well as other effects such as proton migration[10] and hydrogen atom disorder.[11] Other noncovalent interactions have not been as extensively studied as hydrogen bonds. In fact, only a few studies can be found in the literature. Metrangolo et al.[12] have studied the change of A···X−C (A = O, N; X = Br, I) halogen bonds (the interaction of a carbon-bound halogen with Lewis bases) as a function of temperature and showed a qualitative agreement between the magnitude of deformation of the

interactions and the accepted order of interaction strengths O···I−C > N···I−C and N···I−C > N···Br−C.[13]

High-pressure studies on molecular crystals have been used to examine the response of physical properties such as resistivity,[10,14,15] absorption,[10,15,16] luminescence,[17] self-diffusion,[18] or even the properties of impurities in solids.[19] More recently, pressure-driven spin-crossover in the solid state has been observed,[20] and structure−property relationships of magnetic materials under pressure have been studied.[21] Pressure-tuning spectroscopy (infrared, Raman, and electronic) has been widely used for many of these investigations,[22] whereas high-pressure structural studies are less common.[10,20,21,23]

The exploration of high pressure in the study of polymorphism, an area of great interest across a wide range of crystalline materials, appears very promising;[24] elevated pressure has recently been used for the search of new polymorphs,[25] either by inducing phase transitions by applying pressure to a sample[26] or even by crystallizing under pressure.[27] In contrast, less attention has been paid to the effect of pressure within the range of stability of a single polymorph. Similarly to lowering the temperature, noncovalent interactions can also be compressed by instead applying high pressure. This has the clear advantage

(5) For books in the area of crystal engineering, see: (a) *Making Crystals by Design: Methods, Techniques and Applications*; Braga, D., Grepioni, F., Eds.; Wiley: New York, 2006. (b) *Crystal Engineering: From Molecules and Crystals to Materials*; Braga, D., Grepioni, F., Orpen, A. G., Eds.; Kluwer Academic Publishers: Dordrecht, The Netherlands, 1999. (c) *Crystal Engineering. The Design and Application of Functional Solids*; Seddon, K. R., Zaworotko, M., Eds.; Kluwer Academic Publishers: Dordrecht, The Netherlands, 1999. (d) Desiraju, G. R. *Crystal Engineering: The Design of Organic Solids*; Elsevier: Amsterdam, 1989.

(6) For recent general reviews covering crystal engineering involving inorganic systems, see: (a) Brammer, L. *Chem. Soc. Rev.* **2004**, *33*, 476. (b) Janiak, C. *J. Chem. Soc., Dalton Trans.* **2003**, 2781. (c) James, S. L. *Chem. Soc. Rev.* **2003**, *32*, 276. (d) Khlobystov, A. N.; Blake, A. J.; Champness, N. R.; Lemenovskii, D. A.; Majouga, A. G.; Zyk, N. V.; Schröder, M. *Coord. Chem. Rev.* **2001**, *222*, 155. (e) Brammer, L. In *Perspectives in Supramolecular Chemistry*; Desiraju, G. R., Ed.; Wiley: Chichester, 2003; Vol. 7, pp 1−75. (f) Beatty, A. M. *CrystEngComm* **2001**, *3*, 243. (g) Braga, D.; Grepioni, F.; Desiraju, G. R. *Chem. Rev.* **1998**, *98*, 1375. (h) *J. Chem. Soc., Dalton Trans.* **2000**, (21), 3705−3998. (This entire issue is devoted to inorganic crystal engineering).

(7) (a) Already by 1939 the anisotropic thermal expansion of hydrogen-bonded crystals had been observed and its relationship to the different strength of hydrogen bonds in different directions of the crystal had been postulated.[7b](b) Robertson, J. M.; Ubbelohde, A. R. *Proc. R. Soc. London* **1939**, *A170*, 241.

(8) Jeffrey, G. A. *An Introduction to Hydrogen Bonding*; Oxford University Press: New York, 1997; Chapter 2.

(9) Parkin, A.; Adam, M.; Cooper, R. I.; Middlemiss, D. S.; Wilson, C. C. *Acta Crystallogr.* **2007**, *B63*, 303.

(10) (a) Konno, M.; Okamoto, T.; Shirotani, I. *Acta Crystallogr.* **1989**, *B45*, 142. (b) Parkin, A.; Harte, S. M.; Goeta, A. E.; Wilson, C. C. *New J. Chem.* **2004**, *28*, 718. (c) Gilli, P.; Bertolasi, V.; Pretto, L.; Ferretti, V.; Gilli, G. *J. Am. Chem. Soc.* **2004**, *126*, 3845. (d) Wilson, C. C.; Xu, X. L.; Florence, A. J.; Shankland, N. *New J. Chem.* **2006**, *30*, 979. (e) Morrison, C. A.; Siddick, M. M.; Camp, P. J.; Wilson, C. C. *J. Am. Chem. Soc.* **2005**, *127*, 4042. (f) Gilli, P.; Bertolasi, V.; Pretto, L.; Antonov, L.; Gilli, G. *J. Am. Chem. Soc.* **2005**, *127*, 4943. (g) Gilli, P.; Bertolasi, V.; Pretto, L.; Lycka, A.; Gilli, G. *J. Am. Chem. Soc.* **2002**, *124*, 13554.

(11) (a) Wilson, C. C.; Goeta, A. E. *Angew. Chem., Int. Ed.* **2004**, *43*, 2095. (b) Parkin, A.; Seaton, C. C.; Bladgen, N.; Wilson, C. C. *Cryst. Growth Des.* **2007**, *7*, 531. (c) Parkin, A.; Wozniak, K.; Wilson, C. C. *Cryst. Growth Des.* **2007**, *7*, 1393.

(12) Metrangolo, P.; Neukirch, H.; Pilati, T.; Resnati, G. *Acc. Chem. Res.* **2005**, *38*, 386.

(13) Forni, A.; Metrangolo, P.; Pilati, T.; Resnati, G. *Cryst. Growth Des.* **2004**, *4*, 291.

(14) Adachi, T.; Ojima, K.; Kato, K.; Kobayashi, H. *J. Am. Chem. Soc.* **2000**, *122*, 3238.

(15) Takeda, K.; Shirotani, I.; Yakushi, K. *Chem. Mater.* **2000**, *12*, 912.

(16) (a) Zahner, J. C.; Drickamer, H. G. *J. Chem. Phys.* **1960**, *33*, 1625. (b) Tkacz, M.; Drickamer, H. G. *J. Chem. Phys.* **1986**, *85*, 1184.

(17) (a) Drickamer, H. G.; Frank, C. W. *Electronic Transitions and the High-Pressure Chemistry and Physics of Solids*; Chapmann and Hall: London, 1973. (b) Hidvegi, I.; Tuszynski, W.; Gliemann, G. *Chem. Phys. Lett.* **1981**, *77*, 517. (c) Levasseur-Thériault, G.; Reber, C.; Aronica, C.; Luneau, D *Inorg. Chem.* **2006**, *45*, 2379.

(18) (a) Dickerson, R. H.; Lowell, R. C.; Tomizuka, C. T. *Phys. Rev.* **1965**, *137*, A613. (b) Chhabildas, L. C.; Gilder, H. M. *Phys. Rev. B* **1972**, *5*, 2135.

(19) (a) Kelley, C. S. *Phys. Rev. B* **1975**, *12*, 594. (b) Rimai, L.; Deutsch, T.; Silverman, B. D. *Phys. Rev.* **1964**, *133*, A1123.

(20) (a) Guionneau, P.; Marchivie, M.; Garcia, Y.; Howard, J. A. K.; Chasseau, D. *Phys. Rev. B* **2005**, *72*, 214408-1. (b) Granier, T.; Gallois, B.; Gaultier, J.; Real, J. A.; Zarembowitch, J. *Inorg. Chem.* **1993**, *32*, 5305. (c) Guionneau, P.; Brigouleix, C.; Barrans, Y.; Goeta, A. E.; Létard, J.-F.; Howard, J. A. K.; Gaultier, J.; Chasseau, D. *C. R. Acad. Sci.* **2001**, *4*, 161.

(21) Tancharakorn, S.; Fabbiani, F. P. A.; Allan, D. R.; Kamenev, K. V.; Robertson, N. *J. Am. Chem. Soc.* **2006**, *128*, 9205.

(22) Edwards, C. M.; Butler, I. S. *Coord. Chem. Rev.* **2000**, *199*, 1.

(23) Guionneau, P.; Gaultier, J.; Rahal, M.; Bravic, G.; Mellado, J. M.; Chasseau, D.; Ducasse, L.; Kurmoo, M.; Day, P. *J. Mater. Chem.* **1995**, *5*, 1639.

(24) Bernstein, J. *Polymorphism in Molecular Crystals*; Oxford University Press: Oxford, 2002.

(25) Boldyreva, E. V. *Cryst. Growth Des.* **2007**, *7*, 1662.

(26) (a) Katrusiak, A. *Acta Crystallogr.* **1990**, *B46*, 246. (b) Moggach, S. A.; Allan, D. R.; Clark, S. J.; Gutmann, M. J.; Parsons, S.; Pulham, C. R.; Sawyer, L. *Acta Crystallogr.* **2006**, *B62*, 296. (c) McGregor, P. A.; Allan, D. R.; Parsons, S.; Pulham, C. R. *Acta Crystallogr.* **2005**, *B61*, 449. (d) Moggach, S. A.; Allan, D. R.; Parsons, S.; Sawyer, L.; Warren, J. E. *J. Synchrotron Radiat.* **2005**, *12*, 598.

(27) (a) Fabbiani, F. P. A.; Allan, D. R.; Dawson, A.; David, W. I. F.; McGregor, P. A.; Oswald, I. D. H.; Parsons, S.; Pulham, C. R. *Chem. Commun.* **2003**, 3004. (b) Fabbiani, F. P. A.; Allan, D. R.; David, W. I. F.; Moggach, S. A.; Parsons, S.; Pulham, C. R. *CrystEngComm* **2004**, *6*, 504. (c) Fabbiani, F. P. A.; Allan, D. R.; Marshall, W. G.; Parsons, S.; Pulham, C. R.; Smith, R. I. *J. Cryst. Growth* **2005**, *275*, 185. (d) Fabbiani, F. P. A.; Allan, D. R.; Parsons, S.; Pulham, C. R. *CrystEngComm* **2005**, *7*, 179. (e) Oswald, I. D. H.; Allan, D. R.; Day, G. M.; Motherwell, W. D. S.; Parsons, S. *Cryst. Growth Des.* **2005**, *5*, 1055. (f) Katrusiak, A. *Z. Kristallogr.* **2004**, *219*, 669. (g) Katrusiak, A. *Z. Kristallogr.* **2004**, *219*, 573. (h) Fabbiani, F. P. A.; Allan, D. R.; David, W. I. F.; Davidson, A. J.; Lennie, A. R.; Parsons, S.; Pulham, C. R.; Warren, J. E. *Cryst. Growth Des.* **2007**, *7*, 1115.

of overcoming the physical limitations of reducing the temperature, permitting greater compressions of the noncovalent interactions than can be achieved at the lowest accessible temperatures. Therefore, valuable information relating to the interaction potential (and strength) of noncovalent interactions can be obtained by undertaking crystal structure determinations not only over a range of temperatures but also over a range of pressures.[28] For example, Dinnebier and co-workers have studied polymeric alkali metal cyclopentadianides, MCp (M = Li, K, Cs), over a range of pressures (0−3.9 GPa).[29] They conclude that the crystal structures of these compounds are the result of a balance between attractive $M^+ Cp^-$ ionic interactions and carbon−carbon nonbonded repulsion, with no evidence for attractive ligand−ligand interactions.[30] The majority of studies of this type, however, focus only on hydrogen-bonded systems,[31] and only quite recently have a few studies begun to examine the effects of pressure on other noncovalent interactions. Predominantly, these focus on interactions in simple molecular crystals, such as Cl···Cl contacts in CH_2Cl_2,[32] in 1,2,3-trichloropropane,[33] and in *ortho*- and *meta*-chlorobenzenes,[34] Br···Br contacts in CH_2Br_2,[35] I···I contacts in CH_2I_2,[35] S···S contacts in molecular conductors,[23] in L-cysteine,[26b] and in CS_2,[36] and CO···CO contacts in acetone.[37]

The vast majority of the structural studies of crystals under pressure involve purely organic systems or purely inorganic (viz. minerals) substances; only a few examples are found of metal−organic systems. In addition to the previously mentioned work of Dinnebier,[30] Bujak and Angel have found that the $[SbCl_5]^{2-}$ units in crystals of $[(CH_3)_2NH(CH_2)_2NH_3][SbCl_5]$ dimerize into $[Sb_2Cl_{10}]^{4-}$ units at pressures between 0.55 and 1.00 GPa, an effect that cannot be reproduced by lowering the temperature.[38] Not a dimerization but a polymerization was obtained by Allan et al. when they applied a pressure of 4.4 GPa to a single crystal of *cis*-[PdCl₂([9]aneS₃)] where the macrocycle adopts an unprecedented [1233] conformation.[39] A phase transition that occurs with either increasing pressure or decreasing temperature was reported by Casati et al.,[40] who showed that the carbonyl ligands of $[Co_2(CO)_6(PPh_3)_2]$ change from a staggered conformation to eclipsed and that molecular stereochemistry as well as the intermolecular packing can be changed.

The present study provides an outstanding opportunity to interrogate a wide range of intermolecular interactions within

(28) Wood, P. A.; Forgan, R. S.; Henderson, D.; Pidcock, E.; Tasker, P. A.; Parsons, S.; Warren, J. E. *Acta Crystallogr.* **2006**, *B62*, 1099.
(29) 0 GPa indicates atmospheric pressure (i.e., 10^{-4} GPa).
(30) Dinnebier, R. E.; van Smaalen, S.; Olbrich, F.; Carlson, S. *Inorg. Chem.* **2005**, *44*, 964.
(31) (a) Boldyreva, E. V. *J. Mol. Struct.* **2004**, *700*, 151. (b) Katrusiak, A. In *High Pressure Crystallography*; MacMillan, P. F., Katrusiak, A., Eds.; NATO ASI Series 140; Kluwer Academic Press: Dordecht, The Netherlands, 2004; p 513. (c) Katrusiak, A. *Crystallogr. Rev.* **2003**, *9*, 87.
(32) Podsiadło, M.; Dziubek, K.; Katrusiak, A. *Acta Crystallogr.* **2005**, *B61*, 595.
(33) Podsiadło, M.; Katrusiak, A. *Acta Crystallogr.* **2006**, *B62*, 1071.
(34) Bujak, M.; Dziubek, K.; Katrusiak, A. *Acta Crystallogr.* **2007**, *B63*, 124.
(35) Podsiadło, M.; Dziubek, K.; Szafrański, M.; Katrusiak, A. *Acta Crystallogr.* **2006**, *B62*, 1090.
(36) Dziubek, K. F.; Katrusiak, A. *J. Phys. Chem. B* **2004**, *108*, 19089.
(37) Allan, D. R.; Clark, S. J.; Ibberson, R. M.; Parsons, S.; Pulham, C. R.; Sawyer, L. *Chem. Commun.* **1999**, 751.
(38) Bujak, M.; Angel, R. J. *J. Phys. Chem. B* **2006**, *110*, 10322.
(39) Allan, D. R.; Blake, A. J.; Huang, D.; Prior, T. J.; Schröder, M. *Chem. Commun.* **2006**, 4081.
(40) Casati, N.; Macchi, P.; Sironi, A. *Angew. Chem., Int. Ed.* **2005**, *44*, 7736.

Scheme 1. Geometric Descriptions of Types I and II Halogen−Halogen Interactions [a]
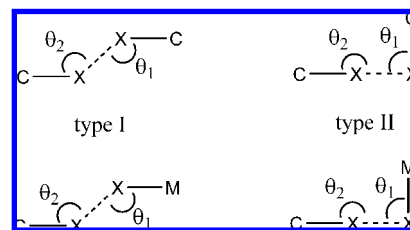
[a] $\theta_1 \approx \theta_2$ for type I; ($\theta_1 \approx 90°$, $\theta_2 \approx 180°$ for type II) for C−X···X−C (top) and M−X···X−C (bottom).

one crystal. Each of the two isostructural compounds studied, (4-chloropyridinium)₂[CoCl₄] (**1**) and (4-chloropyridinium)₂[CoBr₄] (**2**),[41] contains tape motifs propagated via strong N−H···X₂Co hydrogen bonds and Co−X···Cl−C halogen bonds (X = Cl, Br), whereas weaker interactions between tapes include π−π interactions and both Co−X···Cl−C and C−Cl···Cl−C halogen−halogen interactions, which are type I interactions that are both geometrically (Scheme 1) and electronically distinct[42] from the aforementioned halogen bonds (type II).[43] The choice of the two isostructural compounds permits small perturbations to be made to some of the intermolecular interactions through choice of halogen. This approach has been used in a simpler previous study of eight isostructural compounds in which studying the effect on the halogen bond distances of systematically changing the organic (C−X) and inorganic (M−X) halogens allowed us to establish that the main energetic contribution to the M−X···X′−C halogen bonds is the electrostatic rather than charge-transfer contribution.[41]

In the present study, single-crystal X-ray diffraction studies of **1** and **2** each at nine temperatures from 300 to 30 K and at nine pressures from atmospheric pressure to 4.1 GPa for **1** and to 3.7 GPa for **2** have been undertaken.

Experimental Section

Syntheses. Crystals of (4-chloropyridinium)₂[CoCl₄] (**1**) and (4-chloropyridinium)₂[CoBr₄] (**2**) were synthesized as described in ref 41.

X-ray Crystallography at Atmospheric Pressure and Low Temperature. X-ray data at atmospheric pressure were collected for **1** and **2** at nine different temperatures (300, 240, 210, 180, 150, 120, 90, 60, and 30 K) on a Bruker KAPPA APEX II diffractometer, using Mo Kα X-rays. Low temperatures were obtained using an Oxford Cryosystems N-HeliX Cryostat, using N₂ gas flow for the range 300−120 K and He gas flow for the range 90−30 K. Data were corrected for absorption and other systematic errors using empirical methods (SADABS) based upon symmetry-equivalent reflections combined with measurements at different azimuthal

(41) Mínguez Espallargas, G.; Brammer, L.; Sherwood, P. *Angew. Chem., Int. Ed.* **2006**, *45*, 345.
(42) Type II interactions have an attractive electrostatic contribution to their interaction energy arising from the positive polar region of one halogen and the negative equatorial region of the other, whereas type I interactions have either a repulsive or insignificant electrostatic interaction since the regions of interaction on the two halogens are similar ($\theta_1 \approx \theta_2$), although may be weakly attractive due to dispersion forces.
(43) (a) Ramasubbu, N.; Parthasarathy, R.; Murray-Rust, P. *J. Am. Chem. Soc.* **1986**, *108*, 4308. (b) Pedireddi, V. R.; Reddy, D. S.; Goud, B. S.; Craig, D. C.; Rae, A. D.; Desiraju, G. R. *J. Chem. Soc., Perkin Trans.* **1994**, *2*, 2353. (c) Sakurai, T.; Sundralingham, M.; Jeffrey, G. A. *Acta Crystallogr.* **1963**, *16*, 354.

Table 1. Crystallographic Data for Structures **1t1**−**1t9**[d]

	1t1	1t2	1t3	1t4	1t5	1t6	1t7	1t8	1t9
crystal color	blue	blue	blue	blue	blue	blue	blue	blue	blue
crystal system	monoclinic	monoclinic	monoclinic	monoclinic	monoclinic	monoclinic	monoclinic	monoclinic	monoclinic
space group, Z	$C2/c$, 4	$C2/c$, 4	$C2/c$, 4	$C2/c$, 4	$C2/c$, 4	$C2/c$, 4	$C2/c$, 4	$C2/c$, 4	$C2/c$, 4
a (Å)	16.5060(6)	16.4936(9)	16.4930(7)	16.4898(9)	16.4924(6)	16.4836(9)	16.4821(9)	16.4775(9)	16.4754(8)
b (Å)	7.3215(3)	7.3003(4)	7.2802(3)	7.2729(4)	7.2511(3)	7.2469(4)	7.2348(4)	7.2260(4)	7.2193(4)
c (Å)	13.9763(6)	13.8880(9)	13.8389(6)	13.7991(8)	13.7532(5)	13.7167(8)	13.6784(8)	13.6408(8)	13.6161(7)
α (deg)	90	90	90	90	90	90	90	90	90
β (deg)	100.516(2)	100.556(4)	100.550(3)	100.551(3)	100.545(2)	100.551(3)	100.547(3)	100.546(3)	100.541(3)
γ (deg)	90	90	90	90	90	90	90	90	90
V (Å³)	1660.7(1)	1643.9(2)	1633.6(1)	1626.9(2)	1616.9(1)	1610.8(2)	1603.5(2)	1596.7(2)	1592.2(1)
density (Mg/m³)	1.719	1.737	1.748	1.755	1.766	1.772	1.780	1.788	1.793
wavelength (Å)	0.71073	0.71073	0.71073	0.71073	0.71073	0.71073	0.71073	0.71073	0.71073
temp (K)	300(2)	240(2)	210(2)	180(2)	150(2)	120(2)	90(2)	60(2)	30(2)
μ (Mo Kα) (mm⁻¹)	1.984	2.005	2.017	2.026	2.038	2.046	2.055	2.064	2.070
range θ (deg)	2.51−30.46	2.51−30.62	2.51−30.58	2.51−30.67	2.51−30.56	2.51−30.66	2.51−30.61	2.51−30.65	2.51−30.64
completeness (%)	99.7	99.0	99.3	99.1	99.5	99.2	99.6	99.4	99.4
reflns collected	13502	12941	12855	12810	12729	12678	12615	12491	12461
independent reflns, n	2521	2512	2495	2496	2475	2474	2468	2455	2450
(R_{int})	(0.0270)	(0.0279)	(0.0287)	(0.0266)	(0.0257)	(0.0255)	(0.0240)	(0.0235)	(0.0231)
reflns used in refinement	2521	2512	2495	2496	2475	2474	2468	2455	2450
L.S. params (p)	87	87	87	87	87	87	87	87	87
R1(F),[a] $I > 2.0\sigma(I)$	0.0389	0.0335	0.0304	0.0281	0.0255	0.0229	0.0212	0.0205	0.0195
wR2(F^2),[b] all data	0.1094	0.0857	0.0764	0.0698	0.0624	0.0563	0.0564	0.0543	0.0524
$S(F^2)$,[c] all data	1.617	1.564	1.552	1.510	1.489	1.550	1.482	1.553	1.548

[a] R1(F) = $\Sigma(|F_o| - |F_c|)/\Sigma|F_o|$. [b] wR2($F^2$) = $[\Sigma w(F_o^2 - F_c^2)^2/\Sigma wF_o^4]^{1/2}$. [c] $S(F^2)$ = $[\Sigma w(F_o^2 - F_c^2)^2/(n - p)]^{1/2}$. [d] Crystal size: $0.19 \times 0.16 \times 0.10$ mm³.

Table 2. Crystallographic Data for Structures **2t1**−**2t9**[d]

	2t1	2t2	2t3	2t4	2t5	2t6	2t7	2t8	2t9
crystal color	blue	blue	blue	blue	blue	blue	blue	blue	blue
crystal system	monoclinic	monoclinic	monoclinic	monoclinic	monoclinic	monoclinic	monoclinic	monoclinic	monoclinic
space group, Z	$C2/c$, 4	$C2/c$, 4	$C2/c$, 4	$C2/c$, 4	$C2/c$, 4	$C2/c$, 4	$C2/c$, 4	$C2/c$, 4	$C2/c$, 4
a (Å)	17.2842(9)	17.249(1)	17.2461(9)	17.235 (1)	17.243(1)	17.2186(9)	17.2110(9)	17.1969(9)	17.192(1)
b (Å)	7.5139(4)	7.4744(5)	7.4589(4)	7.4456(5)	7.4312(5)	7.4177(4)	7.4028(4)	7.3925(4)	7.3882(4)
c (Å)	14.0608(8)	13.9631(9)	13.9154(8)	13.8804(9)	13.8431(9)	13.8073(7)	13.7689(7)	13.7372(7)	13.7152(8)
α (deg)	90	90	90	90	90	90	90	90	90
β (deg)	100.051(3)	100.123(3)	100.129(3)	100.158(3)	100.143(3)	100.193(2)	100.218(2)	100.243(2)	100.254(3)
γ (deg)	90	90	90	90	90	90	90	90	90
V (Å³)	1798.1(2)	1772.2(2)	1762.1(2)	1753.3(2)	1746.1(2)	1735.7(2)	1726.5(2)	1718.6(2)	1714.2(2)
density (Mg/m³)	2.245	2.278	2.291	2.302	2.312	2.325	2.338	2.349	2.355
wavelength (Å)	0.71073	0.71073	0.71073	0.71073	0.71073	0.71073	0.71073	0.71073	0.71073
temp (K)	300(2)	240(2)	210(2)	180(2)	150(2)	120(2)	90(2)	60(2)	30(2)
μ (Mo Kα) (mm⁻¹)	10.128	10.276	10.334	10.386	10.429	10.492	10.548	10.596	10.623
range θ (deg)	2.39−30.46	2.40−30.55	2.40−30.56	2.40−30.58	2.40−30.55	2.40−30.47	2.40−30.52	2.41−30.55	2.41−30.56
completeness (%)	99.9	99.7	99.9	99.4	99.4	99.9	99.8	99.9	99.5
reflns collected	13008	13157	13048	13000	12958	12860	12790	12761	12197
independent reflns, n	2739	2714	2699	2686	2673	2645	2639	2637	2624
(R_{int})	(0.0232)	(0.0232)	(0.0222)	(0.0219)	(0.0212)	(0.0208)	(0.0207)	(0.0197)	(0.0324)
reflns used in refinement	2739	2714	2699	2686	2673	2645	2639	2637	2624
L.S. params (p)	87	87	87	87	87	87	87	87	87
R1(F),[a] $I > 2.0\sigma(I)$	0.0414	0.0324	0.0280	0.0247	0.0212	0.0181	0.0156	0.0148	0.0188
wR2(F^2),[b] all data	0.1134	0.0837	0.0731	0.0603	0.0495	0.0434	0.0372	0.0352	0.0390
$S(F^2)$,[c] all data	1.674	1.597	1.555	1.444	1.512	1.377	1.337	1.392	1.189

[a] R1(F) = $\Sigma(|F_o| - |F_c|)/\Sigma|F_o|$. [b] wR2($F^2$) = $[\Sigma w(F_o^2 - F_c^2)^2/\Sigma wF_o^4]^{1/2}$. [c] $S(F^2)$ = $[\Sigma w(F_o^2 - F_c^2)^2/(n - p)]^{1/2}$. [d] Crystal size: $0.29 \times 0.20 \times 0.18$ mm³.

angles.[44] Crystal structures were solved and refined against all F^2 values using the SHELXTL suite of programs.[45] Non-hydrogen atoms were refined anisotropically, and hydrogen atoms were placed in calculated positions refined using idealized geometries (riding model) and assigned fixed isotropic displacement parameters. Data collection and refinement statistics are collected in Tables 1 and 2.

X-ray Crystallography at High Pressure and Room Temperature. High-pressure experiments were carried out using a Merrill−Bassett diamond-anvil cell (DAC)[46] equipped with 600-μm culet-cut diamonds and a tungsten gasket with a 300-μm hole. Backing disks were made from beryllium (which is polycrystalline). A 1:1 mixture of pentane and isopentane was used as the pressure transmitting medium, which ensures that pressure is applied hydrostatically. A small chip of ruby was also loaded into the cell

(44) (a) Sheldrick, G. M. *SADABS, Empirical absorption correction program*; University of Göttingen: Göttingen, Germany, 1995; based upon the method of Blessing.[44b] (b) Blessing, R. H. *Acta Crystallogr.* **1995**, *A51*, 33.

(45) Sheldrick, G. M. *Acta Crystallogr.* **2008**, *A64*, 112.

(46) Merrill, L.; Bassett, W. A. *Rev. Sci. Instrum.* **1974**, *45*, 290.

Table 3. Crystallographic Data for Structures **1p1**–**1p9**[d]

	1p1	1p2	1p3	1p4	1p5	1p6	1p7	1p8	1p9
crystal color	blue	blue	blue	blue	blue	blue	blue	blue	blue
crystal system	monoclinic	monoclinic	monoclinic	monoclinic	monoclinic	monoclinic	monoclinic	monoclinic	monoclinic
space group, Z	C2/c, 4	C2/c, 4	C2/c, 4	C2/c, 4	C2/c, 4	C2/c, 4	C2/c, 4	C2/c, 4	C2/c, 4
a (Å)	16.520(3)	16.506(1)	16.499(1)	16.477(1)	16.4411(7)	16.3973(7)	16.356(1)	16.354(5)	16.317(2)
b (Å)	7.310(1)	7.212(1)	7.151(1)	7.071(1)	6.9803(6)	6.8907(7)	6.760(1)	6.577(4)	6.528(2)
c (Å)	13.950(4)	13.752(1)	13.637(1)	13.494(1)	13.3444(6)	13.2377(7)	13.150(1)	13.014(5)	12.914(2)
α (deg)	90	90	90	90	90	90	90	90	90
β (deg)	100.49(2)	100.695(6)	100.808(6)	100.971(6)	101.164(3)	101.387(4)	101.790(5)	102.23(2)	102.46(1)
γ (deg)	90	90	90	90	90	90	90	90	90
V (Å³)	1656.5(6)	1608.7(3)	1580.4(3)	1543.3(3)	1502.5(2)	1466.3(2)	1423.3(3)	1368(1)	1343.1(4)
density (Mg/m³)	1.723	1.775	1.806	1.850	1.900	1.947	2.006	2.087	2.126
wavelength (Å)	0.4880	0.4880	0.4880	0.4880	0.4880	0.4880	0.4880	0.4880	0.4880
temp (K)	300(2)	300(2)	300(2)	300(2)	300(2)	300(2)	300(2)	300(2)	300(2)
pressure (GPa)	0	0.35	0.59	0.85	1.40	1.85	2.60	3.60	4.10
μ (mm⁻¹)	0.684	0.705	0.717	0.734	0.754	0.773	0.796	0.829	0.844
range θ (deg)	2.26–20.42	3.25–20.44	2.87–20.44	3.26–20.49	2.94–20.50	2.96–20.46	2.49–20.41	2.50–20.47	3.07–20.44
completeness (%)	64.3	54.4	54.4	53.8	53.7	53.5	54.3	53.8	52.0
reflns collected	5082	5074	4976	4884	4761	4084	4372	4039	3555
independent reflns, n	1633	1347	1322	1278	1250	1210	1188	1144	1081
(R_{int})	(0.0900)	(0.0612)	(0.0564)	(0.0577)	(0.0618)	(0.1071)	(0.0623)	(0.1078)	(0.0956)
reflns used in refinement	1633	1347	1322	1278	1250	1210	1188	1144	1081
L.S. params (p)	66	66	87	87	87	36	66	36	31
R1(F),[a] $I > 2.0\sigma(I)$	0.0773	0.0578	0.0394	0.0404	0.0402	0.0703	0.0621	0.0790	0.1341
wR2(F^2),[b] all data	0.2972	0.1790	0.1069	0.1037	0.1015	0.2184	0.1904	0.2437	0.3919
S(F^2),[c] all data	0.994	1.240	1.048	1.051	1.060	1.115	1.226	1.060	1.395

[a] R1(F) = $\Sigma(|F_o| - |F_c|)/\Sigma|F_o|$. [b] wR2($F^2$) = $[\Sigma w(F_o^2 - F_c^2)^2/\Sigma w F_o^4]^{1/2}$. [c] S($F^2$) = $[\Sigma w(F_o^2 - F_c^2)^2/(n - p)]^{1/2}$. [d] Crystal size: 0.18 × 0.14 × 0.10 mm³.

to enable pressure measurement by the ruby fluorescence method.[47] X-ray diffraction data were collected for both compounds **1** and **2** at room temperature using synchrotron radiation ($\lambda = 0.4880$ Å) on the three-circle Bruker APEX II diffractometer on Station 9.8 at CCLRC Daresbury Laboratory. Data were collected using ω-scans at eight settings of 2θ and ϕ; full details of the data collection and processing procedures used in this experiment have been given previously.[26d,48] Data integration was performed using the program SAINT[49] with dynamic masking to account for the shading from the DAC steel body. Absorption corrections were carried out in a two-stage procedure using the programs SHADE[50] and SADABS.[44] Crystal structures were solved and refined against all F^2 values using the SHELXTL suite of programs.[45] The completeness of data sets collected at high pressure on samples that belong to low-symmetry crystal systems is invariably quite low because of shading by the cell body, and this is aggravated if the crystal is placed in an unfavorable orientation inside the cell, which cannot readily be controlled. Despite this lack of completeness, all structures could be solved using Patterson methods, but where the free refinement produced a distorted 4-chloropyridinium ring (**1p6**–**1p9**, **2p1**–**2p9**) the distances and angles of the ring were constrained to the values determined at 30 K (i.e., for **1t9** or **2t9**). The assumption is therefore made that intramolecular bond distances and angles within the cation are not greatly affected at pressures up to 4.1 GPa (the highest pressure used in this study). Heavy atoms (Co, Cl, and Br) were refined anisotropically in all the structures except in **1p9**, where one of the chloride ligands was refined isotropically. C and N atoms were refined anisotropically in all cases where the unconstrained refinement of displacement parameters led to physically sensible values (**1p1**–**1p5**, **2p4**–**2p7**, and **2p9**), and isotropically in the others (**1p6**–**1p9**, **2p1**–**2p3**, and **2p8**). H atoms were placed in calculated positions refined using idealized geom-

etries (riding model) and assigned fixed isotropic displacement parameters. Data collection and crystal structure refinement statistics are collected in Tables 3 and 4.

Database Studies. Searches of the Cambridge Structural Database (CSD) were carried out with the program CONQUEST[51] utilizing version 5.29 (November 2007) of the database.

Results

Compounds **1** and **2** form zigzag networks in which the anions are linked by pairs of cations via asymmetrically bifurcated N–H···X₂Co hydrogen bonds and by Co–X···Cl–C halogen bonds (Figure 1). Thirty-six crystal structure refinements are reported, comprising a systematic temperature and pressure study of the two compounds. No phase transitions were observed within the temperature range (300–30 K) and pressure range (0–4.1 GPa for **1** and 0–3.7 GPa for **2**)[29] studied. For all nine temperatures studied for each compound (refinements **1t1**–**1t9** for compound **1**; **2t1**–**2t9** for compound **2**), a full anisotropic refinement was possible based upon an extensive data set. However, restrictions associated with the pressure cell, typical for high pressure studies, limit the completeness of the data set (refinements **1p1**–**1p9** for compound **1**; **2p1**–**2p9** for compound **2**) that can be obtained without remounting the crystal (Tables 3 and 4). Thus, for some refinements, use of isotropic displacement parameters, and/or restraints or constraints on *intra*molecular geometries, was required as is typical for high pressure studies of molecular crystals.[26–28]

The pressures used in this study, up to 4.1 GPa, are unlikely to modify significantly intramolecular geometry of the 4-chloropyridinium ring.[52] Thus, where constraints were needed in structure refinements of some high-pressure structures the model geometry adopted for the chloropyridinium ring was that from

(47) Piermarini, G. J.; Block, S.; Barnett, J. D.; Forman, R. A. *J. Appl. Phys.* **1975**, *46*, 2774.

(48) Dawson, A.; Allan, D. R.; Clark, S. J.; Parsons, S.; Ruf, M. *J. Appl. Crystallogr.* **2004**, *37*, 410.

(49) *SAINT*, version 7; Bruker-AXS: Madison, WI, 2003.

(50) Parsons, S. *SHADE, Program for empirical absorption corrections to high-pressure data*; The University of Edinburgh: Edinburgh, Scotland, 2004.

(51) (a) Allen, F. H. *Acta Crystallogr.* **2002**, *B58*, 380. (b) Allen, F. H.; Motherwell, W. D. S. *Acta Crystallogr.* **2002**, *B58*, 407.

(52) Unconstrained refinement of the cation geometry for structures **1p1**–**1p5** supports this assumption. The change in ring diameter is ca. 1% from structure **1p1** to structure **1p5**.

Table 4. Crystallographic Data for Structures **2p1**−**2p9**

	2p1	2p2	2p3	2p4	2p5	2p6	2p7	2p8	2p9
crystal color	blue	blue	blue	blue	blue	blue	blue	blue	blue
crystal system	monoclinic	monoclinic	monoclinic	monoclinic	monoclinic	monoclinic	monoclinic	monoclinic	monoclinic
space group, Z	$C2/c$, 4	$C2/c$, 4	$C2/c$, 4	$C2/c$, 4	$C2/c$, 4	$C2/c$, 4	$C2/c$, 4	$C2/c$, 4	$C2/c$, 4
a (Å)	17.214(4)	17.211(2)	17.144(4)	17.137(3)	17.082(3)	17.058(2)	17.022(2)	16.968(2)	16.920(3)
b (Å)	7.488(1)	7.3392(4)	7.226(1)	7.188(3)	7.066(2)	7.034(2)	6.978(2)	6.875(2)	6.768(2)
c (Å)	14.009(2)	13.7246(7)	13.553(2)	13.504(2)	13.353(2)	13.273(2)	13.194(2)	13.078(2)	13.009(2)
α (deg)	90	90	90	90	90	90	90	90	90
β (deg)	99.98(2)	100.381(9)	100.61(2)	100.82(1)	101.07(1)	101.103(9)	101.20(1)	101.39(1)	101.54(1)
γ (deg)	90	90	90	90	90	90	90	90	90
V (Å^3)	1778.4(6)	1705.2(2)	1650.1(5)	1634.0(7)	1581.8(6)	1562.7(5)	1537.3(5)	1495.4(5)	1459.6(6)
density (Mg/m^3)	2.270	2.367	2.446	2.470	2.552	2.583	2.626	2.699	2.765
wavelength (Å)	0.4880	0.4880	0.4880	0.4880	0.4880	0.4880	0.4880	0.4880	0.4880
temp (K)	300(2)	300(2)	300(2)	300(2)	300(2)	300(2)	300(2)	300(2)	300(2)
pressure (GPa)	0.09	0.45	0.72	0.90	1.39	1.75	2.20	2.92	3.73
μ (mm^{-1})	3.726	3.885	4.015	4.055	4.189	4.240	4.310	4.430	4.539
range θ (deg)	2.77−20.44	3.04−20.41	3.08−20.38	2.43−20.46	2.47−20.45	2.48−20.47	2.46−20.49	2.48−20.50	2.49−20.51
completeness (%)	41.7	41.6	41.8	57.4	57.8	57.5	57.2	58.6	58.9
reflns collected	5964	5562	5361	5063	4883	4829	4481	4645	4560
independent reflns, n	1141	1090	1053	1447	1406	1383	1358	1352	1333
(R_{int})	(0.0742)	(0.0748)	(0.0646)	(0.0497)	(0.0600)	(0.0426)	(0.0569)	(0.0532)	(0.0629)
reflns used in refinement	1141	1090	1053	1447	1406	1383	1358	1352	1333
L.S. params (p)	36	36	36	67	66	66	66	36	66
R1(F),[a] $I > 2.0\sigma(I)$	0.0623	0.0549	0.0498	0.0520	0.0435	0.0458	0.0514	0.0540	0.0681
wR2(F^2),[b] all data	0.2002	0.1381	0.1391	0.1431	0.1284	0.1408	0.1349	0.1520	0.2036
$S(F^2)$,[c] all data	1.245	1.692	1.160	1.083	1.043	1.297	1.208	1.464	1.439

[a] $R1(F) = \Sigma(|F_o| - |F_c|)/\Sigma|F_o|$. [b] $wR2(F^2) = [\Sigma w(F_o^2 - F_c^2)^2/\Sigma w F_o^4]^{1/2}$. [c] $S(F^2) = [\Sigma w(F_o^2 - F_c^2)^2/(n - p)]^{1/2}$.

the 30 K structure determination (see Experimental Section for full details). Such constraints were not needed for the anion.

Nevertheless, it is the effect of pressure and temperature on *intermolecular* interactions that is the primary focus of the present study. These studies provide a method of probing the repulsive part of the interatomic potential between atoms and between molecules and its influence on molecular packing and intermolecular bonding. These changes are examined systematically in the following sections.

Unit Cell Dimensions. Monotonic changes in unit cell dimensions clearly indicate that no phase transition occurs within the temperature and pressure ranges studied here. A compression of the cell volumes of the crystal structures of compounds **1** and **2** of ca. 5 % was observed when the temperature was lowered from 300 to 30 K (Figure 2b). A larger compression (almost 20% of the cell volume) was achieved by exposing the compounds to high pressure (4.10 GPa (**1**) and 3.73 GPa (**2**)) (Figure 2a).[53]

Although the external effects applied to the crystals are isotropic (temperature and pressure), the variations in the unit cell axes are anisotropic because of the different response of the different types of interactions that take place in each direction (Figure 3). Interestingly, for both **1** and **2** the decrease of temperature produces the greatest compression in the c-axis (ca. 2 %), whereas the greatest reduction occurs in the b-axis (ca. 10 %) upon increasing the pressure.

Since the crystal structures comprise a motif of parallel 1D tapes, it is more instructive to examine the changes in terms of an axial system defined parallel and perpendicular to these tapes. The axial system u, v, and w has been so defined (Figure 4b). The u-axis is parallel to the tapes, and propagation of the structure involves N−H···X$_2$Co hydrogen bonds and Co−X···Cl−C halogen bonds (type II interactions, vide infra). The v-axis involves side-by-side arrangement of the tapes parallel to the aromatic ring planes, and propagation involves type I Co−X···Cl−C halogen−halogen interactions (vide infra). The w-axis corresponds to the crystallographic b-axis along which the tapes are stacked via offset π-π interactions between aromatic rings and via type I C−Cl···Cl−C halogen−halogen interactions.

Looking at the variations along the u, v, and w directions, it is observed that the effects of temperature and pressure differ considerably, and not only in the total compression of the three directions, which, as expected, are larger when increasing the pressure (Figure 5). When cooling to 30 K, maximum compression along the u, v, and w vectors is in the range 1−2% for both **1** and **2**, whereas the u direction is the least compressible of the three directions with pressure (2.52% for **1** at 4.1 GPa, 2.87% for **2** at 3.7 GPa) and the w direction is the most compressible (10.70% for **1** at 4.1 GPa, 9.61% for **2** at 3.7 GPa), indicating differences in behavior for the different intermolecular contacts upon change in pressure and temperature. These
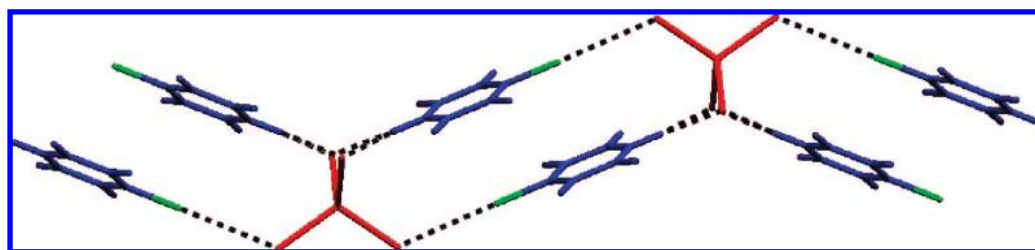

Figure 1. Networks formed in crystal structures of **1** and **2**. Cobalt and halide ligands are shown in red, organic halogens in green, and all other atoms in blue (C, H, N). Black dotted lines represent N−H···X$_2$Co hydrogen bonds and Co−X···Cl−C halogen bonds.
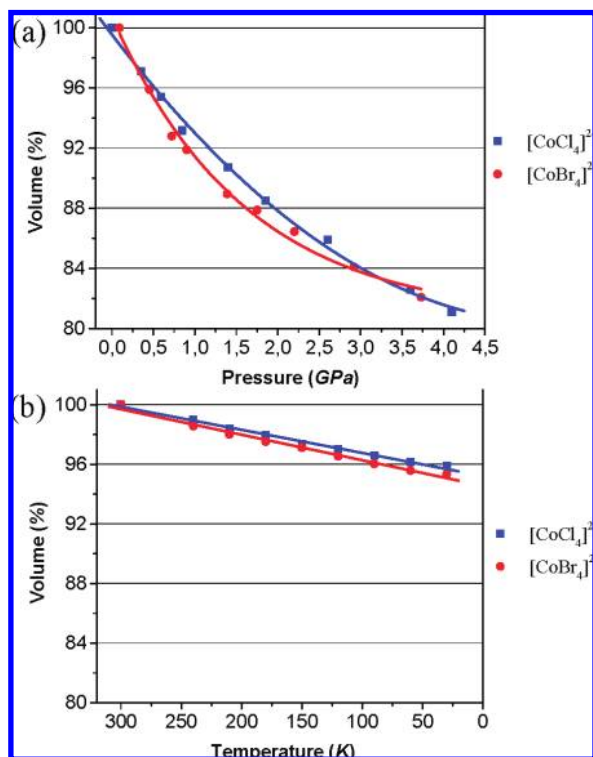
Figure 2. Effect of (a) pressure and (b) temperature on the unit cell volumes of compounds **1** (blue) and **2** (red). The lines serve only as a guide for the eye to trends rather than a quantitative fit to the data.

variations in noncovalent interactions with temperature and pressure are examined in more detail in the following sections. Hydrogen bond and halogen–halogen interaction distances are normalized relative to the corresponding sum of van der Waals radii as suggested by Allen et al. to permit comparison of changes across this range of interactions, particularly upon changing halogens.[57]

Hydrogen Bonds. Metal halides have been shown to be very good hydrogen bond acceptors.[58,59] In the case of tetrahedral halometallate ions, $[MX_4]^{n-}$, it has been shown that the preferential interaction sites for hydrogen bond donors lie along the edges of the tetrahedron, often leading to bifurcated hydrogen bonds $N-H\cdots X_2M$. These interactions are typically asymmetric, and this has been explained as a consequence of the double minimum in the negative electrostatic potential that it is observed along the tetrahedron edge ($X\cdots X$ vector).[59]

Compounds **1** and **2** form asymmetrically bifurcated $N-H\cdots X_2Co$ hydrogen bonds, stronger in the case of $[CoCl_4]^{2-}$ than in $[CoBr_4]^{2-}$ because of the more negative electrostatic potential around the anion in the chlorocobaltate compound.[41,59] As shown in Figure 6, for both compounds **1** and **2** the shorter of the bifurcated $N-H\cdots X_2Co$ hydrogen bonds undergoes very little contraction or compression upon lowering the temperature or increasing the pressure, respectively [variations of 0.00 (**1**) and 0.01 Å (**2**) with temperature and 0.01 (**1**) and 0.05 Å (**2**) with pressure]. The longer of the bifurcated hydrogen bonds, however, is more markedly shortened by both cooling and applying pressure. Interestingly, the hydrogen bonds involving the chloride ligands (**1**) are shortened more than those involving the bromide ligands (**2**) upon both reduction of temperature (from 2.914 to 2.752 Å for **1**; from 2.955 to 2.805 Å for **2**) and upon increase in pressure (from 2.865 to 2.539 Å for **1**; from 2.871 to 2.659 Å for **2**), indicating that the longer of the H bonds is stronger for the bromide ligands than for the chloride ligands [expressed as normalized distances, R_{HX}: upon reducing the temperature (from 0.988 to 0.933 for **1**; from 0.969 to 0.920 for **2**); upon increasing the pressure (from 0.971 to 0.861 for **1**; from 0.941 to 0.872 for **2**)].

Halogen Bonds and Other Halogen⋯Halogen Interactions. As observed for hydrogen bonds, the effect of the applied pressure is greater than that upon temperature reduction for type II (halogen bonds) and type I halogen–halogen interactions. However, the compression of the type I interactions is more pronounced than that of the type II interactions for both compounds **1** and **2** (Figures 7–9).

The $Co-X\cdots Cl-C$ halogen bonds that propagate the tape along the $<10\bar{1}>$ direction (vector *u*) adopt a type II interaction and contract slightly on reduction of temperature from 300 to 30 K [from $Cl\cdots Cl$ distances of 3.382(1) Å (R_{ClCl} = 0.966) to 3.3118(4) Å (R_{ClCl} = 0.946) for **1**, and from $Br\cdots Cl$ distances of 3.531(1) Å (R_{BrCl} = 0.981) to 3.4517(4) Å (R_{BrCl} = 0.959) for **2**]. The rate of decrease ($\Delta d/T$) is constant and similar for the two compounds, as seen in Figure 7b. The effect of increased pressure, apart from greater reduction in the $X\cdots Cl$ distance, differs in rate of change ($\Delta d/p$) for the two compounds, the $(Co)Cl\cdots Cl(C)$ distance (**1**) being less compressible than the $(Co)Br\cdots Cl(C)$ distance (**2**), changing from 3.364(1) Å (R_{ClCl} = 0.961) to 3.130(5) Å (R_{ClCl} = 0.894) for **1**, and from 3.519(3) Å (R_{BrCl} = 0.978) to 3.261(2) Å (R_{BrCl} = 0.906) for **2**.

The $Co-X\cdots Cl-C$ halogen–halogen interactions along the $<101>$ direction (vector *v*) between tapes show a type I

(53) Note: As a comparison, relative to unit cell volumes at room temperature, at 150 K, Pt(dimethylglyoxime)₂ compresses 2.5%;[10] at 30 K [(*E*)-1,2-bis-(4-pyridyl)ethylene]·[1,4-diiodotetrafluorobenzene] compresses 5.0%;[15] at 30 K, [Mn(pyrrol)₃tren] reduces the unit cell volume by 4.7%.[20a] At pressures of ca. 4 GPa, *trans*-[PtCl₂(dms)₂] (dms = dimethyl sulfide) compresses ca. 20%;[54] the Co(III)nitro- and nitritopentamine complexes studied by Boldyreva reduce their volumes ca. 15%;[55] Pt(dimethylglyoxime)₂ compresses 17%;[10] ACp (A = Li, K) compresses 24%;[30] and glycilglycine compresses ca. 15%, in each case relative to volumes at atmospheric pressure.[56]

(54) Hansson, C.; Carlson, S.; Giveen, D.; Johansson, M.; Yong, S.; Oskarsson, Å. *Acta Crystallogr.* **2006**, *B62*, 474.

(55) See summary in Boldyreva, E. V. *J. Mol. Struct.* **2003**, *647*, 159.

(56) Moggach, S. A.; Allan, D. R.; Parsons, S.; Sawyer, L. *Acta Crystallogr.* **2006**, *B62*, 310.

(57) (a) $R_{XCl} = d(X\cdots Cl)/(r_X + r_{Cl})$ and $R_{HX} = d(H\cdots X)/(r_H + r_X)$, where r_X, r_{Cl}, and r_H are, respectively, the van der Waals radii[57b] of halogen X, Cl, and H, following the definition of Lommerse et al.[57c] (b) Bondi, A. J. *J. Phys. Chem.* **1964**, *68*, 441. (c) Lommerse, J. P. M.; Stone, A. J.; Taylor, R.; Allen, F. H. *J. Am. Chem. Soc.* **1996**, *118*, 3108.

(58) (a) Brammer, L.; Bruton, E. A.; Sherwood, P. *Cryst. Growth Des.* **2001**, *1*, 277. (b) Aullón, G.; Bellamy, D.; Brammer, L.; Bruton, E. A.; Orpen, A. G. *Chem. Commun.* **1998**, 653. (c) Mareque Rivas, J. C.; Brammer, L. *Inorg. Chem.* **1998**, *37*, 4756. (d) Lewis, G. R.; Orpen, A. G. *Chem. Commun.* **1998**, 1873. (e) Gillon, A. L.; Lewis, G. R.; Orpen, A. G.; Rotter, S.; Starbuck, J.; Wang, X.-M.; Rodríguez-Martín, Y.; Ruiz-Pérez, C. *J. Chem. Soc., Dalton Trans.* **2000**, 3897. (f) Angeloni, A.; Orpen, A. G. *Chem. Commun.* **2001**, 343. (g) Dolling, B.; Gillon, A. L.; Orpen, A. G.; Starbuck, J.; Wang, X.-M. *Chem. Commun.* **2001**, 567. (h) Felloni, M.; Hubberstey, P.; Wilson, C. C.; Schröder, M. *CrystEngComm* **2004**, *6*, 87. (i) Balamurugan, V.; Hundal, M. S.; Mukherjee, R. *Chem.−Eur. J.* **2004**, *10*, 1683. (j) Adams, C. J.; Crawford, P. C.; Orpen, A. G.; Podesta, T. J.; Salt, B. *Chem. Commun.* **2005**, 2457. (k) Adams, C. J.; Angeloni, A.; Orpen, A. G.; Podesta, T. J.; Salt, B. *Cryst. Growth Des.* **2006**, *6*, 411. (l) Balamurugan, V.; Jacob, W.; Mukherjee, J.; Mukherjee, R. *CrystEngComm* **2004**, *6*, 396. (m) Turner, D. R.; Smith, B.; Goeta, A. E.; Radosavljevic Evans, I.; Tochter, D. A.; Howard, J. A. K.; Steed, J. W. *CrystEngComm* **2004**, *6*, 633. (n) Kumar, D. K.; Das, A.; Dastidar, P. *Cryst. Growth Des.* **2006**, *6*, 216.

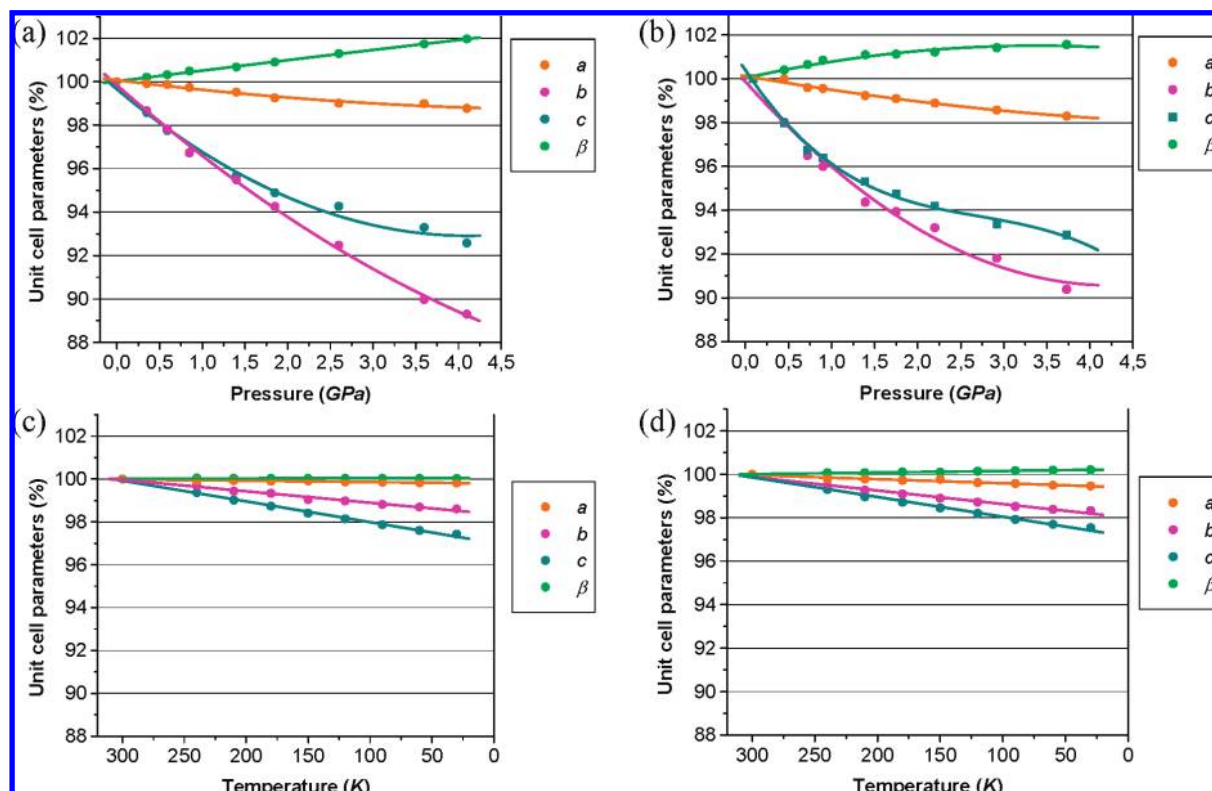(59) Brammer, L.; Swearingen, J. K.; Bruton, E. A.; Sherwood, P. *Proc. Nat. Acad. Sci. U.S.A.* **2002**, *99*, 4956.

Figure 3. Effect of pressure and temperature on the unit cell dimensions of compounds **1** and **2**. Percentage variation with pressure for (a) **1** and (b) **2**. Percentage variation with temperature for (c) **1** and (d) **2**. Lines are a guide to trends as in Figure 2.
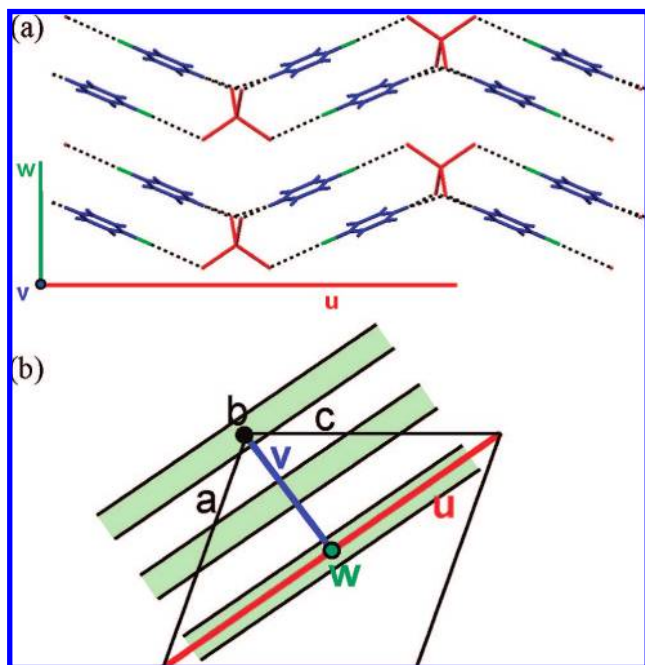

Figure 4. (a) Definition of vectors *u*, *v*, and *w* relative to the tape motifs. (b) Schematic of tape motifs showing vectors *u* <10$\bar{1}$>, *v* <101>, and *w* <010> in relation to the unit cell axes.

geometry; in this case, Co–X···Cl and X···Cl–C angles are close to 90°. Upon lowering the temperature from 300 to 30 K, we find that these Co–X···Cl–C interactions are compressed from Cl···Cl distances of 3.767(1) Å (R_{ClCl} = 1.076) to 3.6399(4) Å (R_{ClCl} = 1.040) for **1**, and from Br···Cl distances of 3.833(1) Å (R_{BrCl} = 1.065) to 3.7026(4) Å (R_{BrCl} = 1.029)

for **2** (Figure 8b), a very similar compression to that noted for the type II Co–X···Cl–C halogen bonds (Figure 7b). However, application of pressure produces a far greater compression of these interactions than that observed for the corresponding type II interactions, from 3.767(5) Å (R_{ClCl} = 1.076) to 3.335(4) Å (R_{ClCl} = 0.953) for **1**, and from 3.861(4) Å (R_{BrCl} = 1.073) to 3.457(2) Å (R_{BrCl} = 0.960) for **2**.

A third type of halogen–halogen interaction occurs between tapes in the <010> direction (*w*-vector). These C–Cl···Cl–C interactions adopt a type I geometry (C–Cl···Cl of ca. 80°). As in the two previous cases, these interactions are slightly compressed with the reduction of temperature, from Cl···Cl distances of 3.708(1) Å (R_{ClCl} = 1.059) to 3.6301(6) Å (R_{ClCl} = 1.037) for **1**, and from Cl···Cl distances of 3.753(2) Å (R_{ClCl} = 1.072) to 3.6845(8) Å (R_{ClCl} = 1.053) for **2** (Figure 9b). The pressure increase again results in a larger compression, comparable with that observed for the type I Co–X···Cl–C interactions [from 3.698(3) Å (R_{ClCl} = 1.057) to 3.317(8) Å (R_{ClCl} = 0.948) for **1**, and from 3.754(2) Å (R_{ClCl} = 1.073) to 3.267(3) Å (R_{ClCl} = 0.933) for **2**].

π–π Stacking. Offset π–π stacking occurs between pairs of cations within the tapes. This interaction lies along the *b*-axis (*w*-vector), the most compressible direction in the crystal structures of compounds **1** and **2**. We have examined the compression of this noncovalent interaction in two ways, studying the variation of the centroid-to-centroid distance with temperature and pressure) as well as the interplanar distance (Figure 11), thereby quantifying interplanar compression as well as slippage. As depicted in Figure 10b, the centroid-to-centroid distance in both compounds **1** and **2** is reduced with temperature by a similar amount for each (from 4.455 to 4.413 Å for **1**, a reduction of 0.042 Å, and from 4.506 to 4.449 Å for **2**, a reduction of 0.057 Å). However, by increasing the pressure the
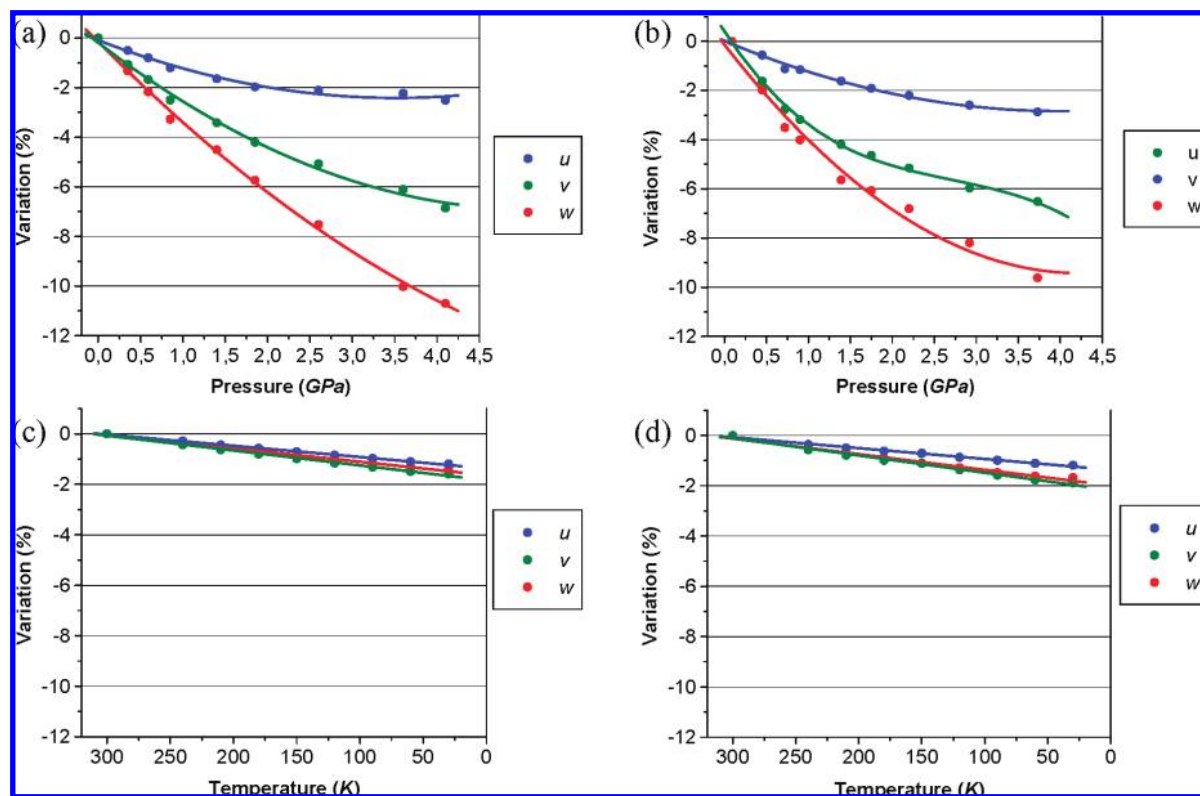
Figure 5. Percentage change in length with pressure along vectors *u*, *v*, and *w* for (a) **1** and (b) **2**. Percentage change in length with temperature along vectors *u*, *v*, and *w* for (c) **1** and (d) **2**. Lines are a guide to trends as in Figure 2.
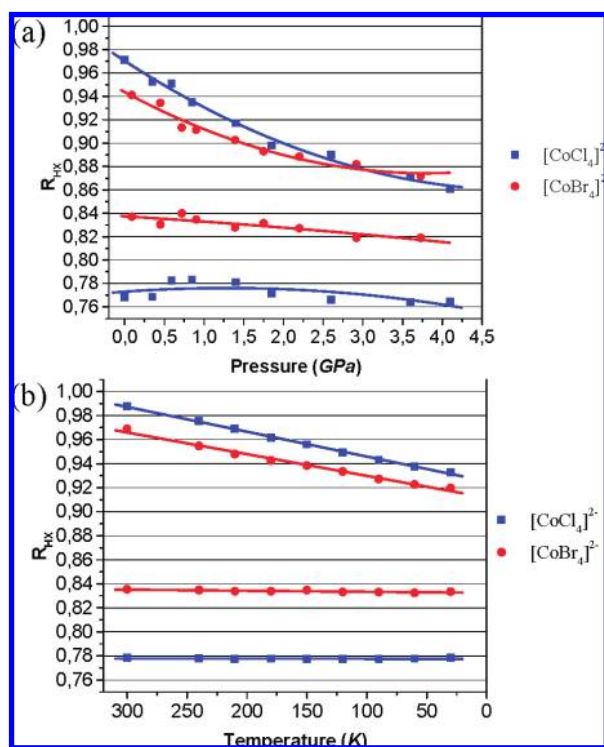

Figure 6. Variation of the two H···X distances in bifurcated N−H···X₂Co hydrogen bond for **1** and **2**. (a) Upon change in pressure and (b) upon change in temperature. Interatomic distances are normalized to permit comparison between **1** and **2** where the halide ligands have different sizes. Lines are a guide to trends as in Figure 2.
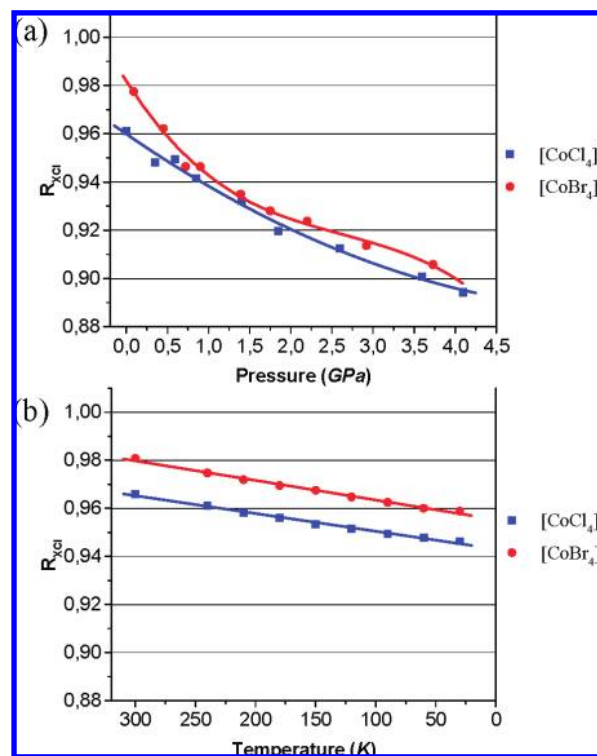
Figure 7. Variation of the (Co)X···Cl(C) halogen bond distances (type II interaction) for **1** and **2**. (a) Upon change in pressure and (b) upon change in temperature. Interatomic distances are normalized to permit comparison between **1** and **2** where the halide ligands have different sizes. Lines are a guide to trends as in Figure 2.
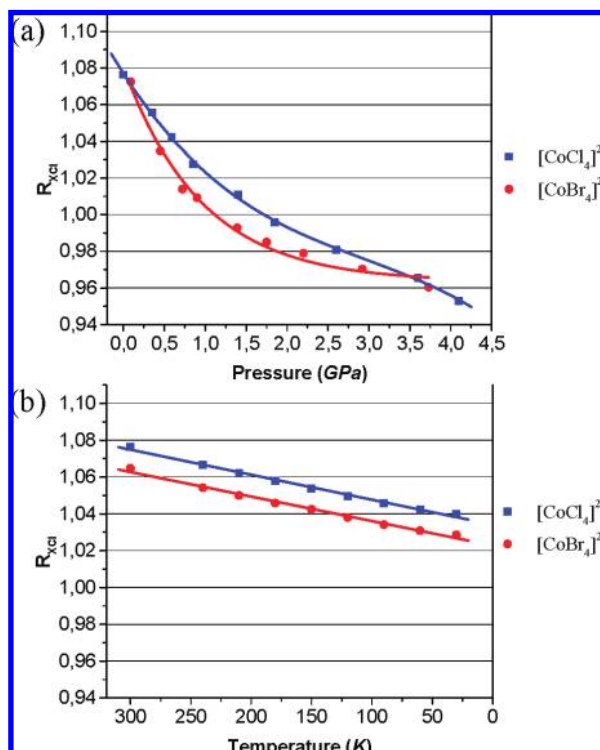
Figure 8. Variation of the type I (Co)X···Cl(C) halogen−halogen interaction distances for **1** and **2**. (a) Upon change in pressure and (b) upon change in temperature. Interatomic distances are normalized to permit comparison between **1** and **2** where the halide ligands have different sizes. Lines are a guide to trends as in Figure 2.

Figure 9. Variation of the type I (C)Cl···Cl(C) halogen−halogen interaction distances for **1** and **2**. (a) Upon change in pressure and (b) upon change in temperature. Interatomic distances are normalized to permit comparison between **1** and **2** where the halide ligands have different sizes. Data shown in blue for **1** and red for **2**. Lines are a guide to trends as in Figure 2.

$\pi-\pi$ stacking in compound **2** is compressed more than that in compound **1** (from 4.467 to 4.207 Å for **1**, a reduction of 0.260 Å, and from 4.502 to 4.231 Å for **2**, a reduction of 0.271 Å upon application of a slightly lower pressure; Figure 10a).

Figure 11a,b shows the variation of the interplanar distances with pressure and temperature, respectively. It can be seen that reduction of the temperature has similar effects on both compounds **1** and **2** (from 3.439 to 3.346 Å for **1**, a reduction of 0.093 Å, and from 3.461 to 3.361 Å for **2**, a reduction of 0.100 Å), while the compression with pressure is larger for compound **1** (from 3.426 to 2.960 Å for **1**, a reduction of 0.466 Å, and from 3.441 to 3.107 Å for **2**, a reduction of 0.334 Å).

Distortion of the Anions. The $[CoX_4]^{2-}$ anions have a tetrahedral geometry that is distorted from the idealized tetrahedral arrangement. Previously, it has been determined that this distortion observed in the anions is the response to the local electric field of the surrounding ions, thereby generating a dipole moment along the twofold axis of the anion.[41] In the crystal structures of **1** and **2** at room temperature and atmospheric pressure, the X−Co−X angle involved in the hydrogen bonding is smaller than that of a tetrahedron, while the X−Co−X angle involved in the halogen bonds is larger, thereby generating a dipole moment that opposes that generated in the vicinity of the anions by the pairs of halopyridinium cations. In the present study, we examined the variation of this distortion upon the reduction of temperature and the increase of pressure. Figure 12 shows that reduction of the temperature results in insignificant changes in all X−Co−X angles. However, when pressure is applied, while the X−Co−X angle involved in the hydrogen bonding also remains essentially constant, the X−Co−X angle involved in the halogen bonding is markedly
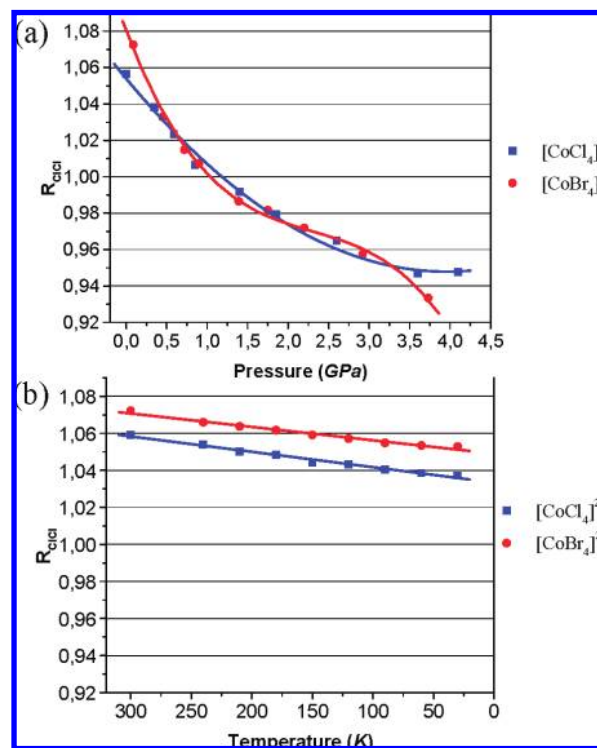
expanded (from 112.6(1)° to 121.6(4)° in **1**, and from 113.4(1)° to 119.5(2)° in **2**).

Discussion

The reduction in temperature and application of pressure is effectively isotropic across the crystals. In contrast, the (geometric) changes that result for the crystal structures of compounds **1** and **2** are quite anisotropic. This anisotropy reflects the different response of different types of noncovalent interactions associated with different directions within the crystal structures. The magnitude of the geometric changes is far less upon reducing the temperature from 300 to 30 K at atmospheric pressure than the effect of increasing the pressure from atmospheric to ca. 4 GPa at room temperature. Nevertheless, the anisotropic response manifests itself in terms of a smaller compression or contraction along a vector parallel to the tape motifs (vector u <10$\bar{1}$>) than that in the directions perpendicular to the tapes (vector v <101> and vector w <010>). The discussion hereafter will focus predominantly upon the changes in the crystal structures arising from application of high pressure since these are the greatest in magnitude and therefore the most revealing regarding the intermolecular interactions in these crystal structures.

Stronger intermolecular interactions are expected to be less easily distorted than weaker interactions, since the former are described by deeper and steeper-sided potential wells, whereas the latter are associated with shallower potential wells. Thus, the anisotropic compression noted is entirely consistent with the stronger interactions being those that propagate the tapes, viz. the bifurcated N−H···X$_2$Co hydrogen bonds and the Co−X···Cl−C halogen bonds (type
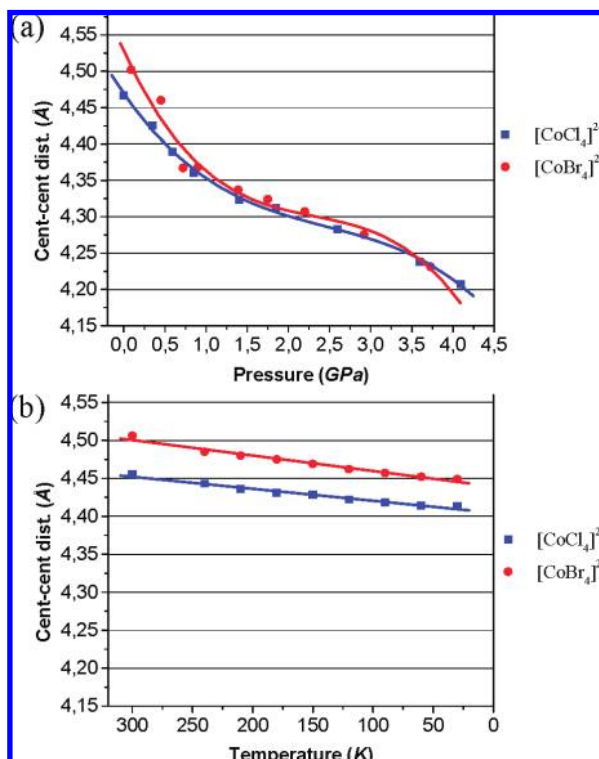
Figure 10. Variation in intratape centroid-to-centroid distances between the pairs of chloropyridinium rings for **1** and **2**. (a) Upon change in pressure and (b) upon change in temperature. Lines are a guide to trends as in Figure 2.
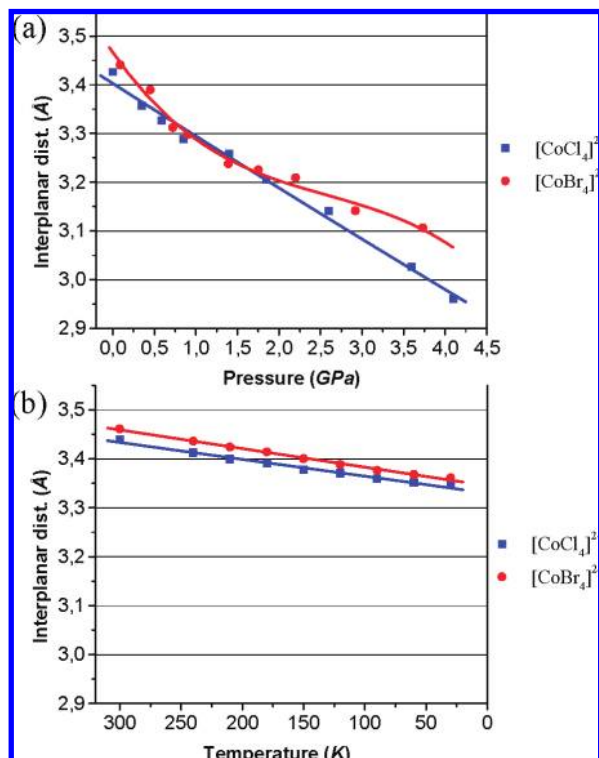

Figure 11. Variation in interplanar distances between the pairs of chloropyridinium rings for compounds **1** and **2**. (a) Upon change in pressure and (b) upon change in temperature. Lines are a guide to trends as in Figure 2.

II geometry). While this may seem unsurprising, it is important that a clear distinction in behavior is made here between the Co–X···Cl–C halogen bonds along the tapes
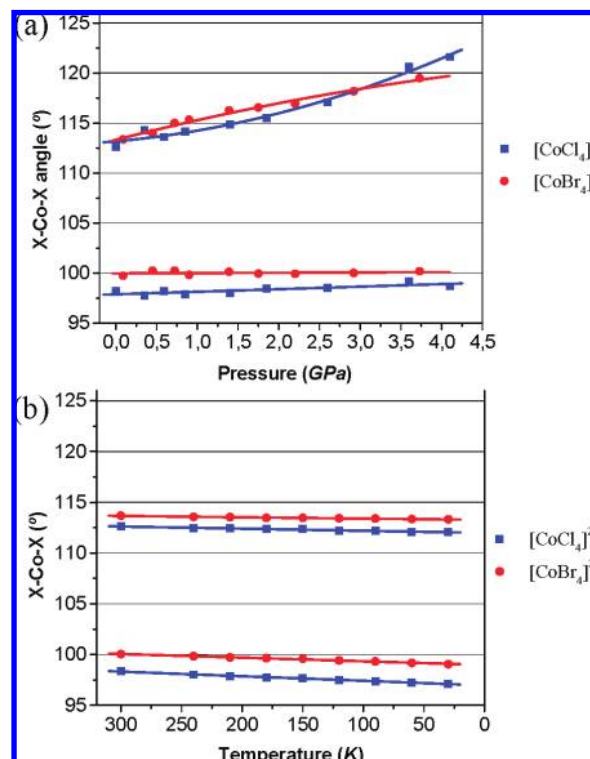
Figure 12. Variation of X–Co–X angles for compounds **1** and **2**. (a) Upon change in pressure and (b) upon change in temperature. In each graph, the upper pair of lines corresponds to the halides involved in halogen bonds, and the lower pair of lines corresponds to the halides involved in the hydrogen bonds. Data shown in blue for **1** and red for **2**. Lines are a guide to trends as in Figure 2.

and the type I halogen–halogen interactions (Co–X···Cl–C and C–Cl···Cl–C) between the tapes (Scheme 1). The specific changes in these interactions together with the changes in π–π stacking and in anion geometry are discussed below.

Hydrogen Bonds. Perhalometallate anions have been extensively studied as hydrogen bond acceptors, and their application in crystal engineering for the design of organic–inorganic hybrid solids has been widely developed in recent years.[58,59] In the case of tetrahedral halometallates, $[MX_4]^{n-}$, it has been found that hydrogen bond donors tend to form bifurcated asymmetric interactions along one edge of the X_4 tetrahedron, involving a shorter interaction with one of the two halides. This has been explained as the result of the double minimum in the negative electrostatic potential along these edges.[59,60] Compounds **1** and **2** form this typical asymmetric bifurcated N–H···X_2Co hydrogen bond under ambient conditions, and this type of hydrogen bond becomes weaker and more symmetric on going from chloride to bromide ligands, since the electrostatic potential around the tetrachlorocobaltate anion is more negative than that for the tetrabromocobaltate.[41]

The compressibility of hydrogen bonds has been well established in organic systems, showing that strong hydrogen bonds cannot be compressed much while weak hydrogen bonds are easily compressed.[27] For compounds **1** and **2**, both

(60) This contrasts with the case for square planar tetrahalometallates, $[MX_4]^{n-}$, which exhibit instead a single minimum in the negative electrostatic potential along the four X···X edges since the smaller X–M–X angle results in overlap of the minima that arises from separate halide ligands.

**Scheme 2.** Variation of the Bifurcated Hydrogen Bonds with Pressure[a]
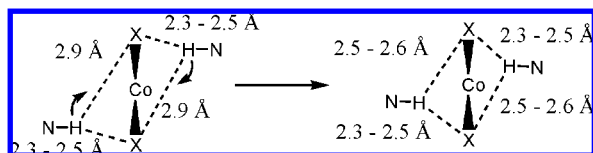
[a] Note that the short interaction does not change while the long one becomes shorter, resulting in a rotation of the N−H group around the tetrahalocobaltate group.

Scheme 3. Anisotropic Exchange Repulsion and Electrostatic Interactions for Interactions of C−X and M−X Groups

short and long hydrogen bonds are present in the bifurcated N−H⋯X_2Co hydrogen bond, and their response to external actions is quite different. As shown in the Results, the short hydrogen bonds are not significantly changed in geometry with change in either temperature or pressure, indicating the strength of this interaction. The longer ones, however, are compressed upon either reducing the temperature or increasing the pressure, indicating that these lie in a shallow region of the interaction potential. This could be due to two factors: (i) the electrostatic potential corresponding to these hydrogen bonds has a shallow potential well, thus corresponding to a weak interaction, or (ii) the potential curve is deep, corresponding to a strong hydrogen bond, but the hydrogen atoms lie at distances beyond the minimum in their potential well. The lack of variation of one of the bifurcated interactions occurring in conjunction with a large change in the other one results in a rotation of the chloropyridinium ring about the perhalocobaltate anion (Scheme 2).

Interestingly, the long hydrogen bonds involving the chloride ligands (**1**) are shortened more than those involving the bromide ligands (**2**) both on reducing the temperature and increasing the pressure, suggesting that the longer of the hydrogen bonds is stronger for the bromide ligands than for the chloride ligands.

Halogen Bonds and Other Halogen⋯Halogen Interactions. Three different types of intermolecular interactions between pairs of halogens have been identified in compounds **1** and **2**, two of the form Co−X⋯Cl−C involving inorganic (Co−X) and organic halogens (C−Cl) and one involving only organic halogens, C−Cl⋯Cl−C. The latter is clearly classified as a type I halogen−halogen interaction (Scheme 1) since the two C−Cl⋯Cl angles have the same values (they are related by a center of inversion) (77−82° for **1**; 81−86° for **2**). The two Co−X⋯Cl−C interactions are classified as follows: one as type II, the halogen bonds that connect anions and cations along the tapes (Co−X⋯Cl (θ_1) ≈ 123−129°, C−Cl⋯X (θ_2) ≈ 169−174° for **1** and **2**), and one as type I between tapes (*v*-vector with Co−X⋯Cl (θ_1) ≈ 125−129°, C−Cl⋯X (θ_2) ≈ 92−97° for **1** and **2**). As compression is greater along *w* than *v*, compression of C−Cl⋯Cl−C interactions (*w*-vector) should be greater than that for type I Co−X⋯Cl−C interactions (*v*-vector), but they are not for **1**. This is simply because the ring planes slide one over the other when pressure is applied, increasing the intertape (C)Cl⋯Cl(C) distance.

There has been much debate about the nature of types I and II geometry interactions. Type II M−X⋯X′−C halogen bonds are strong and electrostatically attractive interactions, where the electrostatic contribution is the main component to the energy term (Scheme 3 and refs 41 and 61). Type I M/C−X⋯X′−C
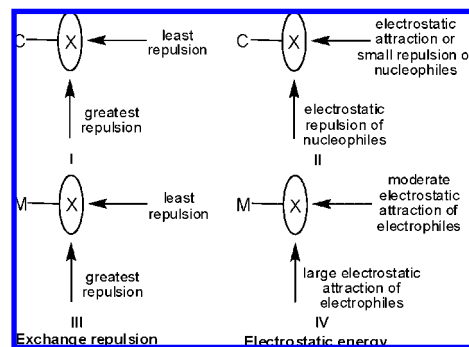
interactions, however, are weak and *electrostatically* repulsive.[62] Thus, similarly to the case of the hydrogen bonds present in **1** and **2**, two types of interactions between halogen atoms are present in these compounds, and their clearly different behavior with pressure provides more evidence on the nature of these interactions.

(a) Type II Co−X⋯Cl−C Halogen Bonds. Complementary chemical environments around the halogens (nucleophilic M−X and electrophilic C−Cl) have been used to develop a new type of synthon with close contacts between halogen atoms. These interactions are stronger for the smaller metal halides and the heavier carbon-bound halogens and consequently, a greater compression might be expected for Co−Br⋯Cl−C halogen bonds than Co−Cl⋯Cl−C halogen bonds. When the temperature is lowered to 30 K, both Co−Br⋯Cl−C and Co−Cl⋯Cl−C halogen bonds are shortened equally. However, the application of pressure shows that the Co−Br⋯Cl−C halogen bond can be compressed more than the chloride analogue, indicating a stronger interaction in the latter case.

With the reduction in temperature and the application of pressure, it might be expected that "super-short" halogen bonds may be obtained (i.e., the shortest M−X⋯Cl−C halogen bonds found in the CSD); however, it is plausible that a lower limit for these contacts exists before a phase transition occurs. A search of the CSD revealed the three shortest M−Cl⋯Cl−C halogen bonds to be 3.113 Å (AMAYAO,[63] where M = Pd), 3.117 Å (NOMGIF,[64] where M = Ru), and 3.133 Å (CPOENR,[65] M = Re), with compounds denoted by their CSD REFCODE. In **1**, the Co−Cl⋯Cl−C distance at 4.10 GPa is 3.130 Å. Thus, we have nearly reached the lower limit observed for such interactions by applying pressure without having a phase transition. The three shortest M−Br⋯Cl−C halogen bonds found in the CSD are 3.336 Å (QEVFOM,[66] M = Ni), 3.348 Å (BOJFOV,[67] M = Re), and 3.371 Å (TEFWOQ,[68] M = Co). When a pressure of 3.73 GPa is applied to compound **2**, an M−Br⋯Cl−C distance of 3.261 Å is observed, which is

(61) Zordan, F.; Brammer, L.; Sherwood, P. *J. Am. Chem. Soc.* **2005**, *127*, 5979.
(62) Price, S. L.; Stone, A. J.; Lucas, J.; Rowland, R. S.; Thornley, A. E. *J. Am. Chem. Soc.* **1994**, *116*, 4910.
(63) Tsoureas, M.; Danopoulos, A. A.; Tulloch, A. A. D.; Light, M. E. *Organometallics* **2003**, *22*, 4750.
(64) Abbenhuis, R. A. T. M.; del Rio, I.; Bergshoef, M. M.; Boersma, J.; Veldman, N.; Spek, A. L.; van Koten, G. *Inorg. Chem.* **1998**, *37*, 1749.
(65) Weiher, U.; Dehnicke, K.; Fenske, D. *Z. Anorg. Allg. Chem.* **1979**, *457*, 115.
(66) Li, F.; Yap, G. P. A.; Scott, S. L.; Ihl Woo, S. *Transition Met. Chem.* **2001**, *26*, 271.
(67) Mronga, N.; Dehnicke, K.; Fenske, D. *Z. Anorg. Allg. Chem.* **1982**, *491*, 237.
(68) Levason, W.; Preece, S. R.; Frampton, C. S. *Polyhedron* **1996**, *15*, 2719.

Scheme 4. Increased Distortion under Pressure of Anion Geometry in Response to Changes in Local Electric Field Generated by Neighboring Ions
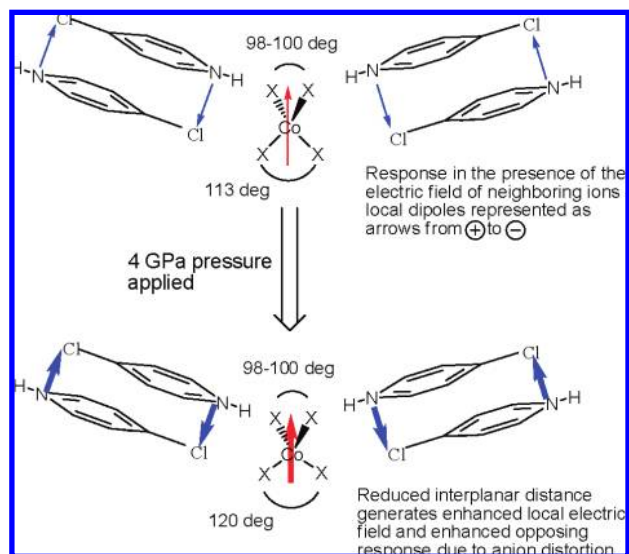
the shortest of the M−Br···Cl−C halogen bonds reported to date at room temperature.

(b) Type I Co/C−X···Cl−C Halogen−Halogen Interactions. The behavior of the type I halogen−halogen interactions is very different to that observed for type II Co−X···Cl−C halogen bonds. Head-to-head contacts between halogens (type I) are electrostatically unfavorable, in contrast to type II Co−X···Cl−C halogen bonds, and they occur as a result of minimizing exchange repulsion energy,[62] with only dispersion forces offering a significant attractive force. Another indication of the different nature of these interactions compared with that of halogen bonds (type II geometry) is that they are shorter when the halide ligand X = Br. The ease with which these interactions are compressed in compounds **1** and **2** is a clear indication of the shallowness of the potential well for the halogen−halogen interactions. This is unexpected since it has been previously calculated that the exchange-repulsion energy varies exponentially with distance, with a cost in energy of 10 kJ mol^{-1} for Cl···Cl separations changing from 3.6 to 3.2 Å.[62]

$\pi-\pi$ Stacking. Compounds **1** and **2** have the aromatic rings centrosymmetrically stacked with one ring laterally offset relative to the other, such that the permanent dipole moments oppose one another, consistent with the Hunter−Sanders model for aromatic ring interactions[69] and with more recent studies of

heteroaromatic compounds by Janiak.[70] The reduction of temperature does not produce major changes in this arrangement. The increase of pressure, on the other hand, produces a substantial decrease of the interplanar distance, with an increase of the repulsive interaction between the negative π-electron clouds. To reduce this repulsive interaction, a further displacement of the offset rings is observed, thus increasing the attractive term. The compression of $\pi-\pi$ stacking interactions with hydrostatic pressure has not been extensively studied. However, it has been reported that the lower limit for compression of phenyl rings is ca. 2.9 Å, and a phase transition occurs once a contact reaches its lower limit.[28] Here we observe that no phase transition occurs as the lower limit is approached, but rather an increase in the offset stacking of the rings occurs.

Distortion of the Anions. The distortion from the idealized tetrahedral arrangement of the $[CoX_4]^{2-}$ anions at atmospheric pressure has been previously postulated to be a response to the local electric field of the surrounding ions, thereby generating a dipole moment along the twofold axis of the anion.[41] In the corresponding crystal structures of **1** and **2**, the X−Co−X angle comprising the halogens involved in hydrogen bonding is smaller than that of a tetrahedron, whereas the X−Co−X angle comprising the halogens involved in the halogen bonds is larger, thereby generating a dipole moment that opposes that of the halopyridinium cations (Scheme 4). The value of local electric field of the surrounding ions is determined by the distance between the two 4-chloropyridinium rings that are hydrogen- and halogen-bonded to the anion. Thus, a change in the geometry of the anion should be observed if a change in this distance is produced.

As seen before, a decrease in temperature does not produce a major change in the distance between the rings. Thus, there is no change in the geometry of the anion since the electric field around the anion is essentially unchanged. By increasing the pressure, however, a significant reduction of the distance between the two halopyridinium rings is observed, with a consequent change in the value of the electric field that they generate. A response of the anion to such a change is observed. To increase the value of the dipole moment that opposes that of the halopyridinium cations, the X−Co−X angle associated with the halogen bonds is enlarged significantly, while the X−Co−X angle associated with the hydrogen bond does not compress, possibly because of a compromise involving optimization of the hydrogen bond geometries.

Internal Pressure. The present study in which two isostructural compounds differing only in the anions, $[CoCl_4]^{2-}$ in **1**

Table 5. Internal Pressure Relationships between Crystal Structures of **1** and **2**

|	unit cell vol (Å^3)	pressure (GPa)	u (Å)	v (Å)	w (Å)
1p1 (Cl)	1657	0	23.482	9.650	7.310
2p3 (Br)	1650	0.72	23.734	9.621	7.226
Δ[**2p3** − **1p1**]	−7	0.72	0.252 (1.06%)	−0.029 (−0.30%)	−0.084 (−1.16%)
1p3 (Cl)	1580	0.59	23.293	9.488	7.151
2p5 (Br)	1582	1.39	23.616	9.479	7.066
Δ[**2p5** − **1p3**]	2	0.80	0.323 (1.37%)	−0.009 (−0.09%)	−0.085 (−1.20%)
1p4 (Cl)	1543	0.85	23.199	9.409	7.071
2p7 (Br)	1537	2.20	23.475	9.385	6.978
Δ[**2p7** − **1p4**]	−6	1.35	0.276 (1.18%)	−0.024 (−0.26%)	−0.093 (−1.33%)
1p5 (Cl)	1502	1.40	23.090	9.320	6.980
2p8 (Br)	1495	2.92	23.380	9.304	6.875
Δ[**2p8** − **1p5**]	−7	1.52	0.270 (1.15%)	−0.026 (−0.28%)	−0.105 (−1.53%)
1p6 (Cl)	1466	1.85	23.018	9.245	6.891
2p9 (Br)	1459	3.73	23.315	9.250	6.768
Δ[**2p9** − **1p6**]	−7	1.88	0.297 (1.27%)	0.005 (0.05%)	−0.123 (−1.82%)
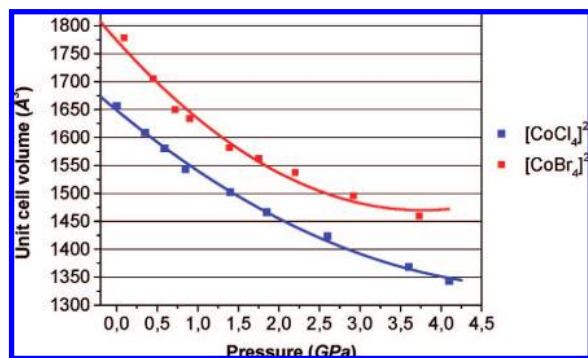
Figure 13. Change of unit cell volume with pressure for **1** and **2**. "Internal pressure" corresponds to the difference (pressure) between the two curves at a common unit cell volume (i.e., the horizontal separation between the two curves).

and $[CoBr_4]^{2-}$ in **2**, provides an unprecedented opportunity to examine the role of "internal" or "chemical" pressure arising from the change of anion. This phenomenon has been reported in studies of organic superconducting salts of the type β-(BEDT-TTF)$_2$Y, whereupon changing the size of the anion, Y, a change in layer spacing occurs, resulting in a change in critical temperature, T_c.[71] Increasing the hydrostatic pressure applied to crystals containing a larger anion to match crystal spacings observed for a smaller anion results in a comparable T_c value. Thus, the β-(BEDT-TTF)$_2$Y salts where Y = AuI_2^- and IBr_2^- show T_c values at atmospheric pressure equivalent to those observed with the larger anion I_3^- at pressures of 0.35 and 0.6 GPa, respectively.[72]

In the context of the present study, five pairs of structures of **1** and **2** exhibit comparable unit cell volumes, permitting a more extensive comparison of internal pressure effects over a range of pressures (Table 5). It is apparent that the internal pressure exerted by changing from $[CoBr_4]^{2-}$ in **2** to $[CoCl_4]^{2-}$ in **1** increases with increasing pressure, although remains approximately constant at ca. 1 GPa for measurements up to 1.5 GPa on **1**.[73] This is consistent with the fact that the rate of compression ($-dV/dp$) decreases at higher pressures (Figure 13). Most informative, however, is the comparison of the changes along the vectors *u*, *v*, and *w* between the pairs of structures for which **1** and **2** have comparable unit cell volumes (Table 5), which shows the effect of internal pressure to be quite anisotropic. Consistently, the dimension *u* is compressed by ca. 1.2% for compound **1** relative to that of **2** and clearly indicates the more attractive nature of the $N-H\cdots Cl_2Co$ hydrogen bonds and $Co-Cl\cdots Cl-C$ halogen bonds over their $N-H\cdots Br_2Co$ and $Co-Br\cdots Cl-C$ counterparts. These compressions are compensated by expansions along the *v* and *w* directions of ca.

0.2 and 1.3%, respectively, consistent with the weaker interactions present along these directions.

Conclusions

The impact upon noncovalent interactions of changes in temperature or pressure provides useful information on the intermolecular interaction potentials in molecular crystals. We have described here the effect of extreme conditions (high pressure and low temperature) on the structures of compounds (4-ClpyH)$_2$[CoX$_4$] (4-ClpyH = 4-chloropyridinium; X = Cl, Br). The most general conclusion is that the effect of quite modest pressures exceeds considerably the structural changes that occur on cooling to low temperature, consistent with studies of other molecular crystals, thus overcoming the physical limitations of reducing the temperature. More importantly, it has been shown that the application of isotropic perturbations such as changes in temperature or pressure produces an anisotropic response of the crystal structures because of the different behavior of noncovalent interactions. Thus, it has been established that the stronger of the interactions present in these crystal structures, the least compressible ones, are $N-H\cdots X_2Co$ hydrogen bonds and $Co-X\cdots Cl-C$ halogen bonds that propagate the tapes, whereas the most compressible direction of the crystal structures corresponds to the direction of the $\pi-\pi$ stacking and type I $C-Cl\cdots Cl-C$ halogen-halogen (dispersion) interactions. The study of the pair of isostructural compounds at multiple pressures uniquely affords the opportunity to examine the effect of the "internal pressure" (chemical pressure) exerted upon changing the $[CoBr_4]^{2-}$ anion in **2** for $[CoCl_4]^{2-}$ in **1**. The effect of making this change is approximately equivalent to the application of 1 GPa pressure on the tetrabromocobaltate-containing crystals. Furthermore, this resultant internal pressure is quite anisotropic such that crystals of **1** and **2** studied at pressures wherein they have equal unit cell volumes exhibit marked contraction along the direction of the tapes for **1** and are expanded in a compensatory manner in other directions. This is clearly indicative that the $N-H\cdots Cl_2Co$ and $Co-Cl\cdots Cl-C$ interactions that propagate the tape are more attractive than their $N-H\cdots Br_2Co$ and $Co-Br\cdots Cl-C$ counterparts in **2**.

Finally, the work presented here has permitted confirmation of the deviation from the idealized tetrahedral geometry that would be expected a priori in the halocobaltate anions as a response to the local electric field generated from the surrounding cations.

Supporting Information Available: Full details of all crystal structure determinations. This material is available free of charge via the Internet at http://pubs.acs.org.

JA8010868

(69) Hunter, C. A.; Sanders, J. K. M. *J. Am. Chem. Soc.* **1990**, *112*, 5525.
(70) Janiak, C. *J. Chem. Soc., Dalton Trans.* **2000**, 3885.
(71) Graja, A. *Phase Transitions* **1996**, *57*, 81.
(72) Schirber, J. E.; Azevedo, L. J.; Kwak, J. F.; Venturini, E. L.; Leung, P. C. W.; Beno, M. A.; Wang, H. H.; Williams, J. M. *Phys. Rev.* **1986**, *B33*, 1987.
(73) Raw pressure measurements indicate an internal pressure of 0.7 GPa for the atmospheric pressure measurement on **1** (**1p1**) rising to 1.88 GPa for the 1.85 GPa measurement of **1** (**1p6**). However, the uncertainty in the pressure measurement is better accounted for in Figure 13, wherein the internal pressure is measured as the horizontal separation between the two curves.